European Journal of Medicinal Chemistry 222 (2021) 113579

Contents lists available at ScienceDirect

European Journal of Medicinal Chemistry

journal homepage: http://www.elsevier.com/locate/ejmech

Structure activity relationship (SAR) study identifies a quinoxaline urea analog that modulates IKKβ phosphorylation for pancreatic cancer therapy

Satish Sagar [a, 1], Sarbjit Singh [a, 1], Jayapal Reddy Mallareddy [a, 1], Yogesh A. Sonawane [a, 1], John V. Napoleon [a], Sandeep Rana [a], Jacob I. Contreras [a], Christabelle Rajesh [a], Edward L. Ezell [a], Smitha Kizhake [a], Jered C. Garrison [c], Prakash Radhakrishnan [a, b, d, e, *], Amarnath Natarajan [a, c, d, e, *]

[a] Eppley Institute for Cancer Research, Omaha, NE, USA
[b] Department of Biochemistry and Molecular Biology, Omaha, NE, USA
[c] Department of Pharmaceutical Sciences, Omaha, NE, USA
[d] Department of Genetics Cell Biology and Anatomy, Omaha, NE, USA
[e] Fred & Pamela Buffett Cancer Center, University of Nebraska Medical Center, Omaha, NE, USA

ARTICLE INFO

Article history:
Received 5 April 2021
Received in revised form
19 May 2021
Accepted 22 May 2021
Available online 30 May 2021

Keywords:
Quinoxaline urea
IKKβ
NFκB
Pancreatic cancer

ABSTRACT

Genetic models validated Inhibitor of nuclear factor (NF) kappa B kinase beta (IKKβ) as a therapeutic target for KRAS mutation associated pancreatic cancer. Phosphorylation of the activation loop serine residues (S^{177}, S^{181}) in IKKβ is a key event that drives tumor necrosis factor (TNF) α induced NF-κB mediated gene expression. Here we conducted structure activity relationship (SAR) study to improve potency and oral bioavailability of a quinoxaline analog 13−197 that was previously reported as a NFκB inhibitor for pancreatic cancer therapy. The SAR led to the identification of a novel quinoxaline urea analog **84** that reduced the levels of p-IKKβ in dose- and time-dependent studies. When compared to 13−197, analog **84** was ~2.5-fold more potent in TNFα-induced NFκB inhibition and ~4-fold more potent in inhibiting pancreatic cancer cell growth. Analog **84** exhibited ~4.3-fold greater exposure ($AUC_{0-\infty}$) resulting in ~5.7-fold increase in oral bioavailability (%F) when compared to 13−197. Importantly, oral administration of **84** by itself and in combination of gemcitabine reduced p-IKKβ levels and inhibited pancreatic tumor growth in a xenograft model.

1. Introduction

Nitrogen containing heterocycle quinoxaline derivatives are associated with varied applications [1], including being part of several approved drugs, such as the smoking cessation agent Varenicline [2], Brimonidine that exhibits antiglaucoma activity [3,4], the antibacterial agent Quinacillin [5], macrocyclic anti-infectives Voxilaprevir, Grazoprevir and Glecaprevir that target hepatitis C virus NS3/4A protease [6,7], and the anticancer agent Erdafitinib that inhibits fibroblast growth factor receptor [8,9]. Although rare the quinoxaline core is also found in macrocyclic DNA-binding quinomycin antibiotics, echinomycin and triostin A [10,11]. The differential π electron density determined by molecular orbital calculations among the three sets of (5,8 > 6,7 > 2,3) carbon atoms on the quinoxaline core, allows extensive derivatization of the core. Quinoxaline analogs have also been explored as antiangiogenic agents, DNA targeting agents, topoisomerase II inhibitors and kinase inhibitors [12]. Our high throughput screening campaigns identified a quinoxaline analog as a hit [13,14]. Follow-up iterative synthesis and screening led us to a quinoxaline analog (13−197), an orally bioavailable IKKβ inhibitor that exhibited anti-cancer activity

* Corresponding author. Eppley Institute for Cancer Research, University of Nebraska Medical Center, 986805 Nebraska Medical Center, BCC 5.12.390, Omaha, NE 68198, USA.
* Corresponding author. Eppley Institute for Cancer Research, University of Nebraska Medical Center, 986805 Nebraska Medical Center, BCC 8.12.321, Omaha, NE 68198, USA.
E-mail addresses: pradhakr@unmc.edu (P. Radhakrishnan), anatarajan@unmc.edu (A. Natarajan).
[1] Equal contribution.

https://doi.org/10.1016/j.ejmech.2021.113579
0223-5234/

in multiple cancer models [15–21].

IKKβ is a member of the IKK complex that regulates the TNFα activated canonical NFκB pathway, which is implicated in chronic inflammatory diseases and cancer [22–24]. The presence of TNFα in the tumor microenvironment of ~50% of surgically resected samples suggests constitutive activation (ca) of the canonical NFκB pathway in these tumors [25]. In Kras mutation-driven cancers, tissue-specific elimination of IKKβ resulted in stalling of the disease in the premalignant state resulting in increased survival of mice [26–28]. In contrast, the introduction of ca-IKKβ in the presence of oncogenic insults such as mutant Apc or Kras enhances tumorigenesis resulting in a dramatic reduction in the median survival of mice, suggesting that ca-IKKβ supports oncogenesis [29–31].

Activation of IKKβ results in the rapid phosphorylation of its endogenous substrate IκBα, resulting in its ubiquitination by beta-transducin repeat containing E3 ubiquitin ligase (β-TrCP) followed by proteasomal degradation [32,33]. The primary role of IκBα in cells is to sequester NFκB in the cytoplasm, therefore TNFα induced degradation of IκBα results in nuclear translocation and expression of NFκB regulated genes [34,35].

Dysregulation of TNFα-induced IKKβ-mediated NFκB activation in pathological conditions led to the development of an array of small molecules and biologics against proteins in this pathway, including five TNFα blockers and three proteasome inhibitors that block the degradation of IκBα approved by the FDA [36–41]. The majority of these inhibitors target NFκB-DNA binding and the second in that list are IKK and IκBα phosphorylation inhibitors, such as ML-120B, TPCA1 and BMS345541 developed by pharmaceutical companies [42–44]. The development of ML-120B and TPCA1 stalled due to unexpected toxicity upon systemic administration [28,45,46]. This provides the impetus for the development of non-toxic small molecules that modulate IKKβ function and inhibit TNFα-induced NFκB activation.

Here we used a cell-based luciferase reporter assay that specifically responds to TNFα stimulation to induce IKKβ-mediated NFκB activity to conduct hit-to-lead optimization of a quinoxaline analog 13–197. Despite the remarkable *in vivo* anti-cancer effects exhibited by 13–197 it suffers from poor oral bioavailability [15–18]. We addressed the above with a structure activity relationship (SAR) study that resulted in the identification of analog **84** that was ~2.5-fold more potent in TNFα-induced NFκB inhibition. Analog **84** was ~4-fold more potent in inhibiting pancreatic cancer cell growth compared to 13–197. We also observed that **84** had ~4.3-fold greater exposure ($AUC_{0-\infty}$) resulting in ~5.7-fold increase in oral bioavailability (%F) when compared to 13–197. Importantly, oral administration of **84** by itself and in combination of gemcitabine reduced p-IKKβ levels and inhibited pancreatic tumor growth in a xenograft model.

2. Results and discussion

2.1. Synthesis of 2,3 disubstituted symmetrical quinoxaline analogs

The synthesis of quinoxaline analogs **38**–**53** are summarized in Scheme 1. Symmetrical diones (**1**) were refluxed with 4-nitrobenzene-1,2-diamine (**2**) in ethanol to generate 2,3-substituted nitro quinoxaline analogs **3**–**6**. Reduction of compounds **3**–**6** under hydrogen atmosphere over Pd/C yielded the corresponding amines **7**–**10** [47]. Condensation of the 2,3-substituted quinoxaline amines with substituted phenyl isocyanates resulted in quinoxaline urea analogs **38**–**39**, **42**–**45** and **47**–**53** in moderate to excellent yields. Furan and phenyl substituted quinoxaline amines **7** and **10** were condensed with 4-bromophenylacetic acid to generate 2,3-substituted quinoxaline amide analogs **40** and **46**, respectively [48]. The thiourea analog **41** was synthesized by condensation of 2,3-di(furan-2-yl)quinoxalin-6-amine **7** with phenyl isothiocyanate in DCM [49].

2.2. Synthesis of mono-substituted quinoxaline analogs

Scheme 2 summarizes the synthesis of key common intermediates 2-chloro-7-nitroquinoxaline (**13**) and 2-chloro-6-nitroquinoxaline (**22a**) required for the synthesis of the mono-substituted quinoxaline analogs **54**–**84** and **86**–**91**. Regioisomers **13** and **22a** were synthesized in 2-steps from commercially available 2-quinoxalinol [50]. Under weakly acidic conditions, the 7-position of 2-quinoxalinol (**11**) is susceptible to electrophilic nitration to yield 7-nitroquinoxalin-2-ol (**12**). The regioselectivity is dictated by the nitrogen atom at the 4-postion of 2-quinoxalinol. Nitration of **11** using the strong acid H_2SO_4 results in protonation of the tautomer quinoxalin-2(1*H*)-one resulting in nitration at the 6-position to yield 6-nitroquinoxalin-2-ol (**22**). Here the regioselectivity is dictated by the OH group at the 2-position. The OH in **12** and **22** were replaced with Cl using $POCl_3/PCl_5$ to yield the key intermediates 2-chloro-7-nitroquinoxaline (**13**) and 2-chloro-6-nitroquinoxaline (**22a**), respectively. The regioselective nitration was confirmed by X-ray crystal structures of compounds **13** and **22a** (Figure S1).

Scheme 3 summarizes the synthesis of mono-substituted quinoxaline analogs **54**–**84**, **86**–**91** and a quinoline analog **85**. Suzuki coupling of **13** and **22a** with different boronic acids/esters resulted in analogs **14**–**17** and **23**–**26** respectively [51]. Palladium catalyzed hydrogenation of **14**–**17** and **23**–**26** yielded the corresponding amines **18**–**21** and **27**–**30**, respectively. Quinoxaline urea analogs **54**–**61**, **70**, **72**, **75**–**84** and **86** were synthesized either by condensation of quinoxaline amines **18**–**21** with different isocyanates or by generating quinoxaline isocyanates from **18**–**21** followed by the addition of the corresponding amines. Addition of various isocyanates to the quinoxaline amines **27**–**30** yielded the quinoxaline urea analogs **62**–**69**, **71** and **73**–**74**. Fused quinoxaline urea analogs (**88**–**92**) were generated by the addition of corresponding isocyanates to analog **21**. A Skraup-type reaction of 4-nitroaniline with 2,2,3-tribromopropanal gave 3-bromo-6-nitroquinoline (**32**). Suzuki coupling of **32** followed by reduction yielded the pyrazole derivative **34**. The quinoline isocyanate was generated from **34** and condensed with 3-bromo-4-fluoroaniline to yield the pyrazolo-quinoline analog **85**.

2.3. Structure activity relationship study with quinoxaline and quinoline analogs

The library of 55 quinoxaline and quinoline analogs were screened in a cell-based luciferase reporter assay that specifically reports on TNFα-induced NFκB activation (Fig. 1A). The compounds were screened at 10 μM with 13–197 and the allosteric IKKβ inhibitor BMS345541 as controls. The substitutions on the 2,3 disubstituted quinoxaline analogs (**38**–**53**) was well tolerated and changes did not have a significant effect on the inhibition of TNFα-induced IKKβ-mediated NFκB activity. All of them exhibited ~15–45% inhibition of the activity, which was comparable to that of 13–197. Among the mono-substituted quinoxaline analogs, the *N*-methyl pyrazole substituted analogs **76**–**78**, showed significant improvement in activity. Replacing the electron donating $-OCH_3$ and OCF_3 at the meta-position of **77** and **78** with CF_3 in analog **79** resulted in further improvement of activity. The meta-Cl and para-F disubstituted analog **80** was ~3-fold more potent than 13–197. Replacing the Cl in analog **80** with a CH_3 in analog **81** dramatically reduced the activity. The activity was restored when an OCH_3 in **82** replaced the CH_3 in **80** and further improved with a OCF_3 substitution in **83**. Incorporating a F atom to the ortho position in analog

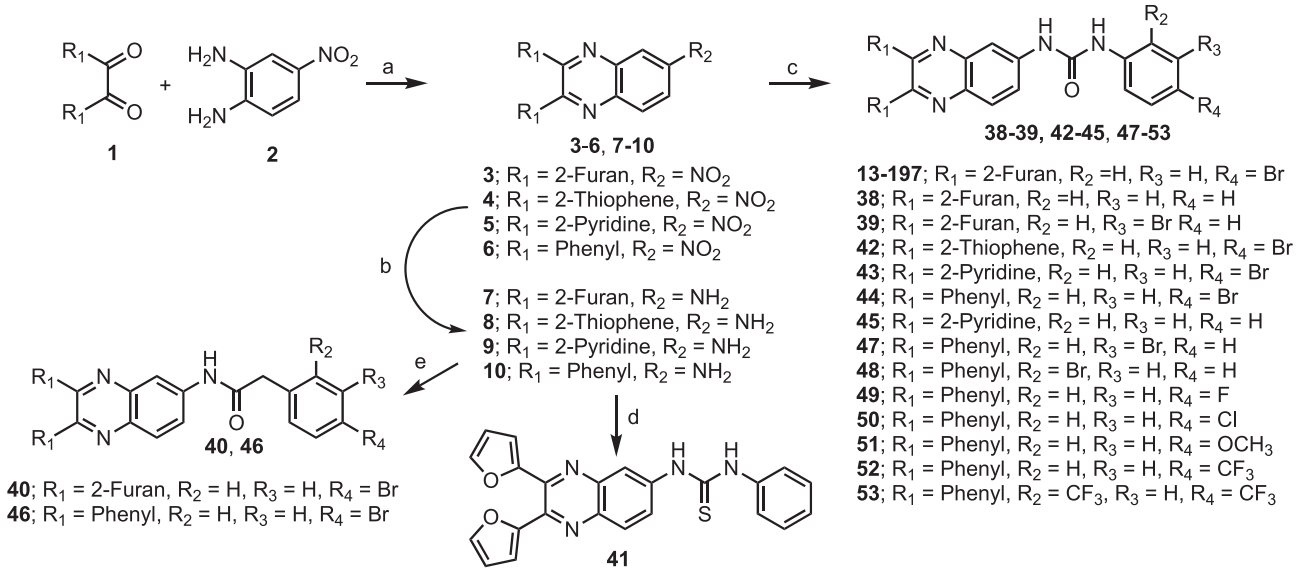

Scheme 1. Reagents and conditions: (a) Ethanol, reflux, 85–99%; (b) H_2/Pd–C, EtOH, rt, 85–96%; (c) Isocyanate derivatives, CH_2Cl_2, rt, 62–83%; (d) Phenyl isothiocyanate, DIPEA, CH_2Cl_2, rt, 70%; (e) 4-Bromophenylacetic acid, EDC, DIPEA, CH_2Cl_2, rt, 62–83%.

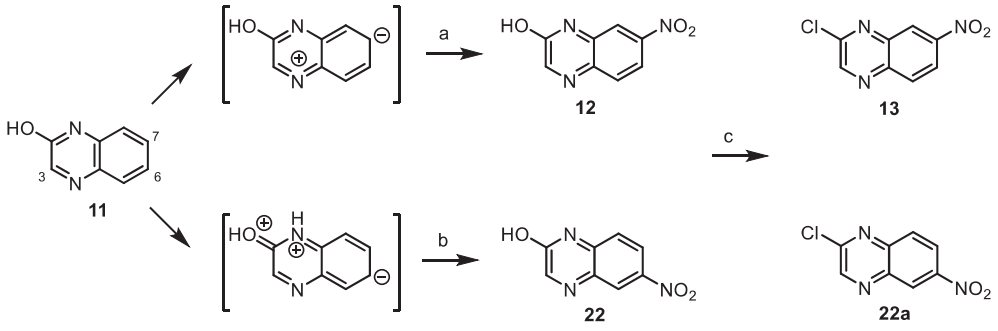

Scheme 2. Reagents and conditions: a) Acetic acid, conc. HNO_3, rt, 24 h, 85%; (b) $NaNO_3$, H_2SO_4, 0°C-rt, 2 h, 88%; (c) PCl_5, $POCl_3$, 110 °C, 12 h, 90%.

79 yielded the most potent inhibitor in analog **84**. When compared to **84**, changing the core to a quinoline in **85** or replacing the *N*-methylpyrazole with an *N*-methylpyrrole in **86** resulted in loss of activity. The three most potent inhibitors were the disubstituted analogs **79**, **80** and **84**; however, incorporating a cyclic structure to replace the di-substitution in analogs **87**–**91** resulted in a significant loss of activity. Together our SAR identified the quinoxaline urea, *N*-methylpyrazole and an electron-deficient phenyl as the key elements required for inhibiting TNFα-induced IKKβ-mediated NFκB activity. Analog **84** with an *o*-F, *m*-CF_3 substituted phenyl quinoxaline urea was the most potent inhibitor.

The activation of caspases, a class of cysteine proteinases, is routinely used by us and others as indicators for the induction of apoptosis [20,40,41,52–55]. We assessed the ability of *N*-methylpyrazole quinoxaline analogs (**78**–**81**, **83** and **84**) along with 13–197 and BMS345541 to activate effector caspases 3/7 in pancreatic cancer (MiaPaCa2) cells (Fig. 1B). The cells were subjected to 10 μM of the 8 compounds and incubated for 24 h and caspase 3/7 activation was assessed using a luminescence assay. The results showed that analog **84** most potently induced caspase activation. This is consistent with the inhibition of TNFα-induced NFκB activity and **84** was found to be ~4-fold more potent than 13–197. Moreover, we observed remarkable correlation ($R^2 = 0.74$) between the ability of the compounds to induce caspase 3/7 and inhibit TNFα-induced NFκB activity (Fig. 1C).

The absolute configuration of **84** was assigned using 1D and 2D NMR spectroscopy. ^{1}H NMR taken in DMSO-d_6 showed a singlet at 3.9 ppm corresponding to H-6 of *N*–CH_3. Three singlets at 9.1, 8.6 and 8.3 ppm correspond to the protons adjacent to nitrogen atoms of the quinoxaline (9.1 ppm) and pyrazole rings (8.6 and 8.2 ppm). The doublets appearing at 8.2 ppm (J = 2.2 Hz) and 7.9 ppm (J = 8.9 Hz) correspond to H-10 and H-13 due to their respective meta and ortho couplings with H-12. The doublet of doublets at 7.6 ppm correspond to H-12 (J = 9.0, 2.3 Hz) due its coupling with H-13 and H-10. The multiplets at 8.4 and 7.3 ppm are of H-22 and H-23/24, respectively. Whereas, the exchangeable protons at 9.6 and 9.0 correspond to amidic NH-17 and NH-20, respectively. The quantitative ^{13}C NMR of **84** taken in DMSO-d_6 showed a doublet at 149.9 and 148.2 ppm corresponding to C-26 due to its coupling with an attached fluorine atom (J^{CF} = 252 Hz). On the other hand, C-25 appears as a quartet of doublets at 116 ppm due to its long-range couplings with fluorine atoms present on C-26 and C-28.^{13}C-HMBC NMR showed interactions of amidic NH-17 with C-10 and C-12. Whereas, another amidic NH-20 showed interactions with carbonyl C-18 as well as with C-22 and C-26 confirming that fluorine atom is substituted ortho to NH-20. The appearance of C-25 as doublet of quartet suggests C-25 and C-26 are adjacent to each other (Fig. 1D).

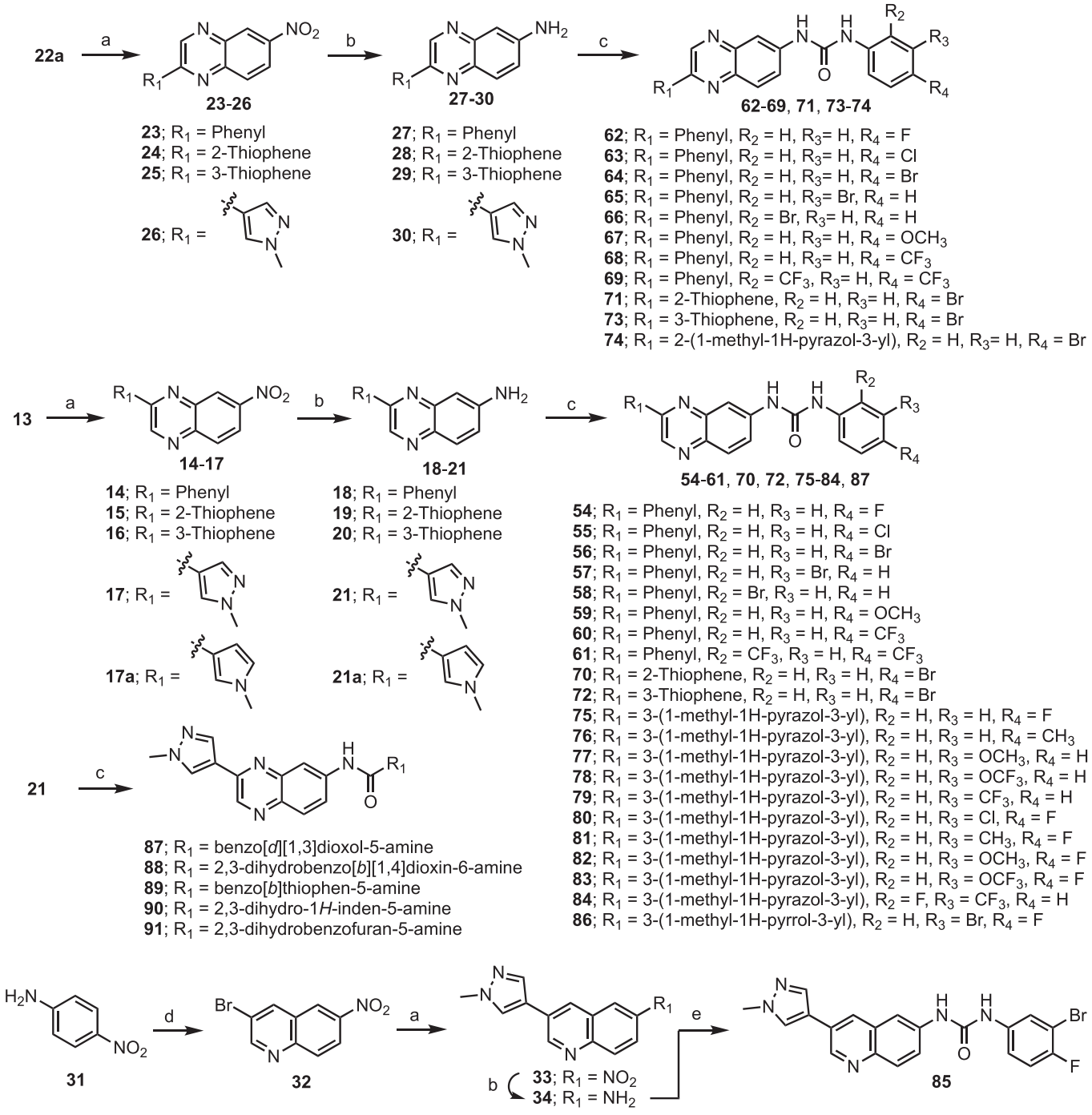

Scheme 3. Reagents and conditions: a) Boronic acids or esters, $Pd(PPh_3)_4$, Na_2CO_3, DMF:Dioxane (1:1), 100 °C, 20 h, 48–88%; (b) Pd/C, H_2, EtOH, 18 h, 88–92%; (c) either (i) BTC, DIPEA, amines, CH_2Cl_2:THF (4:1), rt or (ii) Isocyanates, CH_2Cl_2, rt, 1–3 days, 55–74%; (d) 2,2,3,-tribromopropanal, Glacial acetic acid, 110 °C, 38%; (e) 3-Bromo-4-fluoroaniline, triphosgene, DIPEA, DCM, rt, 32%.

2.4. Characterization of **84** in cell-based assays

In a follow-up experiment, we show that analog **84** inhibited TNFα-induced IKKβ-mediated NFκB activity in a dose-dependent manner and had an IC_{50} value (3.3 ± 0.5 μM) that was ~2.5-fold greater than the reported value for 13–197 (8.4 ± 1.2 μM) (Fig. 2A) [16]. Next, we conducted dose-response and time-course studies to assess the ability of analog **84** to modulate IKKβ function (Fig. 2B). We found that analog **84** reduced the levels of phosphorylated IKKβ in a dose-dependent and a time-dependent manner with low-μM potency. In a 3-day cell growth assay analog **84** inhibited the growth of pancreatic cancer cell lines (MiaPaCa2 and T3M4) with low-μM potency (Fig. 2C). Consistent with caspase 3/7 activation, in a live/dead assay, analog **84** induced MiaPaCa2 cell death in a dose-dependent manner (Fig. 2D). The ability of cancer cells to form colonies is assessed by crystal violet staining in clonogenic assays [56]. Analog **84** inhibited MiaPaCa2 colony forming ability by > 50% when compared to DMSO treated cells (Fig. 2E). Pancreatic cancer is highly metastatic and wound healing assays are used to assess the ability of compounds to inhibit

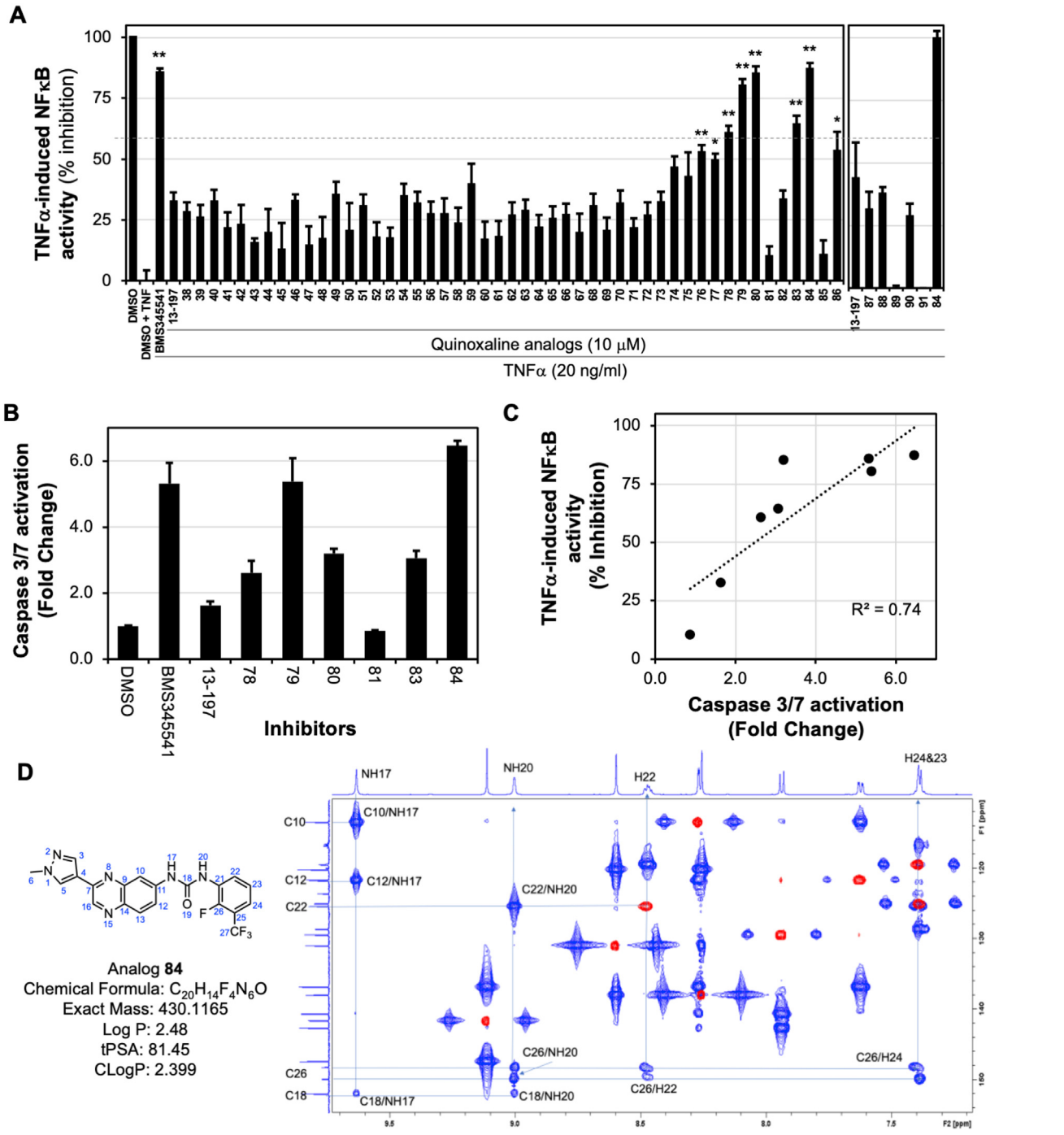

Fig. 1. SAR study identifies **84** as an inhibitor of TNFα-induced NFκB. (A) Quinoxaline and quinoline analogs screened for inhibition of TNFα-induced NFκB activity in a cell-based (A549) luciferase reporter assay. The data is normalized to viability and reported as Ave ± SEM (n = 4), *p-value < 0.05, **p-value < 0.005. (B) MiaPaCa2 cells were treated with analogs **78**–**81**, **83** and **84** along with 13–197 and BMS345541 for 24 h. Apoptosis assessed by measuring the induction of caspase 3/7 activity using Caspase-Glo® 3/7 system (n = 3). (C) Correlation plot derived from the inhibition of TNFα-induced NFκB activity and induction of caspase 3/7 activity by quinoxaline analogs. (D) ^{13}C-HMBC spectra of **84** (blue) overlapped on ^{13}C-HSQC (red).

migration of cells [57]. In a time course study, when compared to DMSO treated cells analog **84** was more effective inhibiting the migration of PDAC cells (Fig. 2F). Together our data shows that analog **84** reduced the levels of phosphorylated IKKβ which results in the inhibition of TNFα-induced NFκB activity. Moreover, analog **84** inhibited cancer cell growth, induced apoptosis, inhibited colony formation and migration of PDAC cells. Our SAR studies have identified analog **84** that does not possess the metabolically labile furan groups and is ~3–4 fold more potent than 13–197 in multiple cell-based assays.

2.5. Pharmacokinetic studies with 13–197 and analog **84**

Furan rings are susceptible to oxidation resulting in the generation of electrophilic intermediates which could lead to toxic and carcinogenic effects [58]. We previously showed that 13–197 had

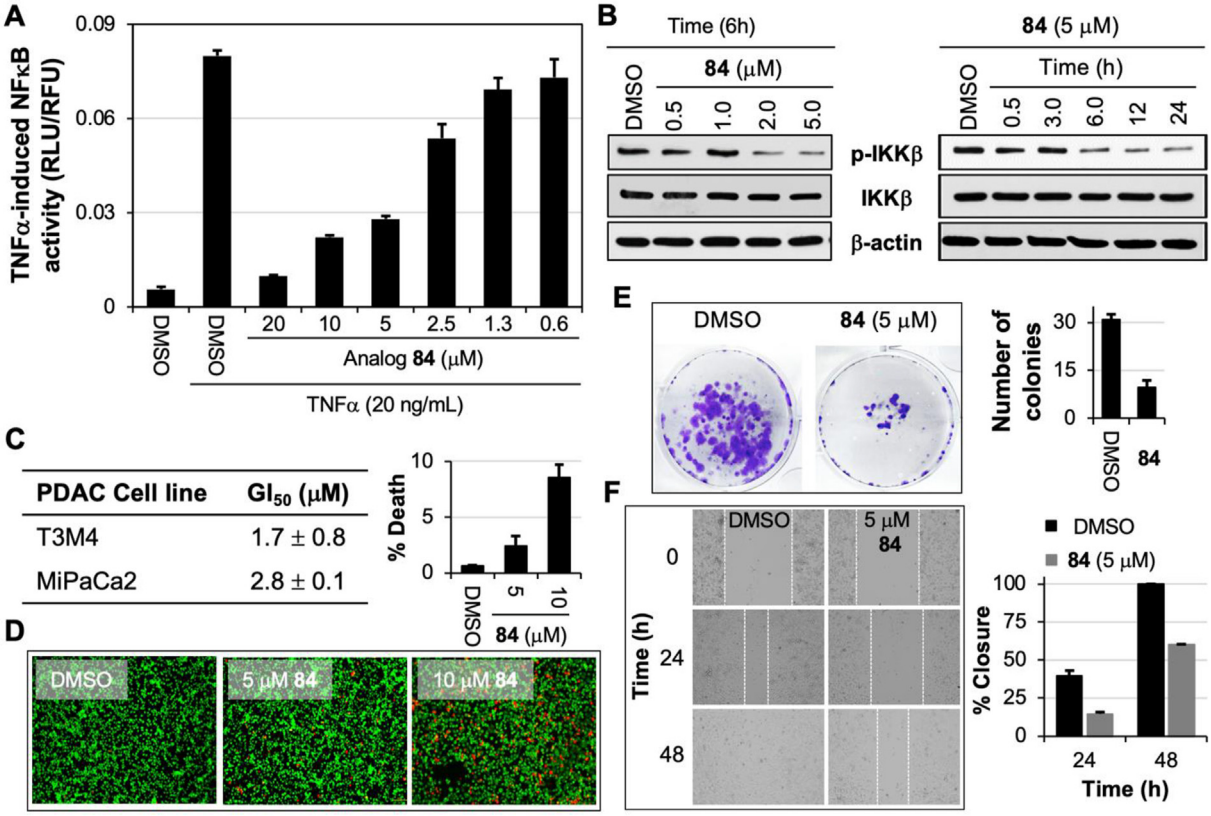

Fig. 2. Evaluation of **84** in PDAC cells. (A) Dose-response study with analog **84** in a dual luciferase reporter assay to assess the inhibition of TNFα-induced IKKβ mediated NFκB activation (n = 3). (B) Dose-response and time-course studies to assess the effect of analog **84** on the activated IKKβ in pancreatic cancer cells. Cell lysates were subjected to Western blotting and probed using the indicated antibodies. β-actin serves as loading control (C) Growth inhibition studies with analog **84** in pancreatic cancer cell lines. Cell viability was determined using PrestoBlue following incubation of compounds for 72 h (n = 3). (D) Live and dead cell assay with analog **84** treated (5 and 10 μM for 24 h) MiaPaCa2 cells (n = 3). (E) Colony formation assay with analog **84** treated (5 μM) MiaPaCa2 cells (n = 3). (F) Scratch assay with analog **84** treated (5 μM at 24 and 48 h) MiaPaCa2 cells (n = 3). All data represented as Ave ± SEM.

oral bioavailability's (%F) of 3 and 16% in mice and rats, respectively. This was attributed to the identification of >20 metabolites and excretion of <1% of intact 13–197 suggesting extensive metabolism of 13–197 [17]. Like 13–197, analog **84** obeys the Lipinski's rule of 5, which suggested > 90% chance that **84** would be orally bioavailable [59]. To determine if replacing the furan rings in 13–197 with a metabolically stable *N*-methylpyrazole resulted in improved %F we conducted PK studies with 13–197 and analog **84**. Mice were orally dosed with 20 mg/kg of 13–197 or **84** and sampled at 0.083, 0.25, 0.5, 1, 2, 4, 8, and 24 h. PK parameters summarized in Table 1 shows that 13–197 and **84** had similar $T_{1/2}$, however the T_{max} and C_{max} for **84** was ~2.5 times greater than that of 13–197. Although this did not have a significant effect on the mean residence time of **84**, it resulted in ~4.3-fold greater exposure ($AUC_{0-\infty}$) when compared to 13–197. To assess oral bioavailability, mice were intravenously dosed with 10 mg/kg of **84** and sampled at the times described above. At half the oral dose the intravenous exposure ($AUC_{0-\infty}$) of **84** was ~2.8-fold higher resulting in an oral bioavailability of 17.6%. In summary, replacing the metabolically labile furan rings in 13–197 with *N*-methylpyrazole and replacing the bromine atom with a $-CF_3$ and fluorine on the phenyl ring in **84** resulted in a ~5.7-fold increase in oral bioavailability (%F).

2.6. *In vivo efficacy studies with analog **84** in pancreatic cancer model*

The cellular efficacy data along with the improved oral bioavailability exhibited by analog **84** prompted us to explore **84** as an anticancer agent in a pancreatic tumor model. Gemcitabine is used as a first line therapy for pancreatic cancer patients therefore we also assessed **84** in a combination setting with gemcitabine. Briefly, MiaPaCa2 cells (2.5×10^6 cells with Matrigel, 2:1 ratio) were subcutaneously implanted in the flanks of athymic nude mice. 20 days after implantation, mice were randomized and distributed into the following treatment groups (n = 6/group): Vehicle (100 μl); **84** (40 mg/kg); Gemcitabine (15 mg/kg) and **84** + Gemcitabine. **84** was dosed orally once a day, Gemcitabine was administered intraperitoneally (*i.p.*) every 3 days. Tumor growth was monitored every 3-days and mice were sacrificed after 4-week treatment (Fig. 3A). At the end of the 4-weeks, when compared to vehicle treated mice gemcitabine alone showed ~45% reduction in tumor volume and tumor weight while **84** alone showed ~75% reduction in tumor volume and tumor weight (Fig. 3B). More importantly mice treated with combination of gemcitabine and **84** showed a >90% reduction in tumor volume and tumor weight when compared to the vehicle treated mice. We observed reduction in Ki67 staining in treated mice indicating a reduction in the proliferation index (Fig. 3C). We also observed reduction in p-IKKβ levels in the treated samples indicating modulation of the target by **84** in an *in vivo* setting (Fig. 3D). Together these results show that **84** is an orally bioavailable anticancer agent, combined with gemcitabine is a novel therapeutic option for pancreatic cancer.

Table 1
Pharmacokinetic studies with 13−197 and analog **84**.

Inhibitor	**13-197**	**84**	**84**
Dose (mg/kg)	20	20	10
Route of administration	Oral	Oral	Intravenous
PK Parameters			
$T_{1/2}$ (h)	2.0 ± 0.2	2.5 ± 0.3	2.7 ± 0.9
T_{max} (h)	2.5	6.0	
Cmax (ng/mL)	300 ± 62	700 ± 320	5978 ± 765
AUC_{last} (h*ng/mL)	1628 ± 664	7986 ± 3675	20346 ± 6739
AUC0-∞ (h*ng/mL)	1860 ± 577	8008 ± 3696	22804 ± 4704
MRT 0-∞ (h)	5.2 ± 0.6	6.3 ± 0.5	4.5 ± 0.3
V_{ss} (L/kg)	-	-	2.0 ± 0.4
Bioavailability (%F)	3.1*	17.6	

*Gautam et al, (2013) Biomed. Chromatogr.

3. Conclusion

Phosphorylation mediated constitutive activation of IKKβ has been implicated in enhancing tumorigenesis in the presence of oncogenic insults in multiple cancer models. Phosphorylated IKKβ has also been associated with ~50% of all cancers; therefore, agents that reduce the levels of phosphorylated IKKβ offer a novel therapeutic option. Here, we used a cell-based mechanism specific assay to conduct hit-to-lead optimization studies that identified a novel quinoxaline analog **84** as an inhibitor of TNFα-induced IKKβ-mediated NFκB activity. Among quinoxaline analogs we show an excellent correlation between their ability to inhibit TNFα-induced IKKβ-mediated NFκB activity and the induction of caspase 3/7 activity. In pancreatic cancer cells, analog **84** in a dose- and time-dependent manner reduces p-IKKβ levels, induced apoptosis, inhibits cell growth, colony formation and migration, at low-μM concentrations. Replacing the metabolically labile furan groups in 13−197 with *N*-methylpyrazole in **84** resulted in ~5.7-fold increase in orally bioavailability. Most importantly analog **84** alone and in combination with gemcitabine reduced p-IKKβ levels resulting in a >90% reduction of tumor volume and tumor growth in a xenograft pancreatic mouse model. In summary, we present **84** as a suitable pre-therapeutic anticancer agent that is ideal for lead optimization studies.

4. Experimental methods

4.1. Chemistry

4.1.1. General procedures

All reagents were purchased from commercial sources and were used without further purification. Pre-coated ANALTECH uniplate was used for Thin layer chromatography (TLC) and monitored under UV light at 254 nm and with potassium permanganate stain. Silica gel (230−400 mesh, grade 60, Fisher scientific, USA) was used for Column chromatography. ^{1}H NMR and ^{13}C NMR spectra were recorded in chloroform-d or DMSO-d_6 on a Bruker-400, Bruker-500 and Bruker-600 spectrometer. The purity of final compounds was determined by analytical HPLC and was found to be ≥ 95% pure. Analysis of sample purity was performed on a Waters Alliance 2695 HPLC system Phenomenex Luna-2 RP-C18 (5 μm, 4.6 mm × 250 mm, 120 Å, Torrance, CA) column. HPLC conditions: solvent A, H_2O containing 0.1% formic acid (FA); solvent B, CH_3CN containing 0.1% FA; gradient, 10% B to 100% B over 15 min followed by 100% B over 4 min with flow rate, 1 mL/min. Mass spectrometric data was acquired using Quattro Micro triple quadrupole mass spectrometer with electron-spray ionization (ESI) technique and as TOF mass analyzer. HRMS data was generated on an Agilent 6230 LC/TOF system with UV detector (254 nm).

4.1.2. Synthesis

4.1.2.1. General methods

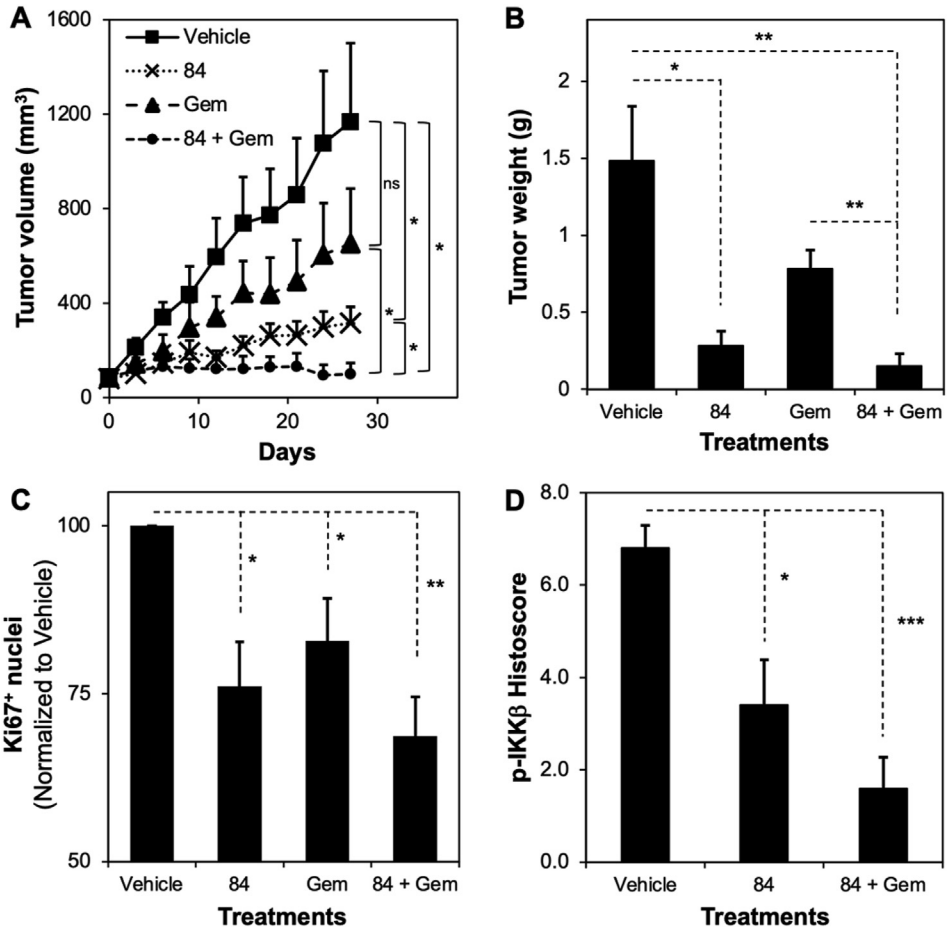

Fig. 3. Tumor growth studies with **84** and gemcitabine. (A) MiaPaCa2 cells were subcutaneously implanted in nude mice and treated with **84** (40 mg/kg, P·O.) or gemcitabine (15 mg/kg i.p.) or the combination and tumor growth monitored for 4-weeks (n = 6). (B) Tumor weights measured at the end of the study. (C) Ki67 staining indicates proliferation index in tumor tissue (n = 5). (D) Levels of p-IKKβ in the tumor tissue indicates *in vivo* target modulation (n = 5). All the data represented as average ± SEM. *P < 0.05, **P < 0.005 and ***P < 0.0005.

4.1.2.1.1. General procedure of Suzuki coupling (Method A). Respected halide (1 eq), Na_2CO_3 (4 eq) in DMF:Dioxane (1:1) and water (0.2 mL) were taken a round bottom flask. The mixture was sonicated and degassed for 5 min by passing nitrogen through it. Degassing was followed by addition of $Pd(Ph_3)_4$ (0.05 eq) and corresponding boronic acids or esters (1 eq). The reaction mixture was stirred under inert atmosphere overnight at 100 °C and quenched by addition of water. The precipitates formed were filtered and triturated in THF and hexane (70–88%).

4.1.2.1.2. General procedure of reduction of nitro compounds to amines (Method B). Respected quinaxoline-nitro compound (1 eq) was dissolved in EtOH followed by the addition of Pd/C (10% w/w) under inert conditions. The reaction mixture was stirred under H_2 atmosphere for 4–12 h at room temperature. After completion of reaction, the mixture was filtered through Celite and solvent was evaporated under reduced pressure to yield corresponding quinaxoline-amine which were used without purification for next transformations (85–99%).

4.1.2.1.3. General procedure of synthesis of urea analogs (Method C). To a suspension of respected quinaxoline amine (1 eq) in DCM was added corresponding isocyanate (1.5 eq). The reaction mixture was stirred for 24–48 h at room temperature. Product was filtered and washed with DCM, hexane and dried under vacuum (55–88%).

4.1.2.1.4. General procedure of synthesis of urea analogs (Method D). Compound **21, 21a,** or **34** was dispersed in THF and diisopropylethylamine (2 eq) and added slowly to a solution of BTC (0.35 eq) in dichloromethane at 0 °C. The mixture was further stirred for 3–6 h until the starting material disappears. A mixture of corresponding amine (1.5 eq) and diisopropylethylamine (2 eq) was added to this mixture and reaction was stirred for next 10–24 h at room temperature. After completion of reaction, the crude was purified by column chromatography using MeOH and DCM as eluting system (55–88%).

Compounds **3**–**10**, **12**–**13**, **22**, **22a**, **38**–**39** and **41**–**45** have been reported previously [19,20,50]. Compounds **14**–**17a, 23**–**26** were synthesized according to Method A and compounds **18**–**21a, 27**–**30** were synthesized according to Method B described in general methods. Compounds **47**–**81, 84, 86** and **88**–**92** were synthesized according to Method C described in general methods. Compounds **82**, **83** and **87** were synthesized according to Method D described in general methods.

*4.1.2.1.5. 7-Nitro-2-(thiophen-2-yl)quinoxaline (**15**).* Yield = 51%; ^{1}H NMR (500 MHz, Chloroform-*d*) δ 9.36 (s, 1H), 8.96 (d, J = 2.6 Hz, 1H), 8.46 (dd, J = 2.5, 9.1 Hz, 1H), 8.21 (d, J = 9.1 Hz, 1H), 7.95 (dd, J = 1.1, 3.8 Hz, 1H), 7.66 (dd, J = 1.1, 5.0 Hz, 1H), 7.34–7.16 (m, 1H); ^{13}C NMR (125 MHz, $CDCl_3$) δ 149.5, 148.6, 145.1, 143.8, 141.5, 141.3, 131.7, 131.0, 129.0, 128.6, 125.5, 122.6; HRMS (ESI-MS) calcd for $C_{12}H_8N_3O_2S^+$ *m/z* $(M + H)^+$ 258.0332, found: 258.0338.

*4.1.2.1.6. 7-Nitro-2-(thiophen-3-yl)quinoxaline (**16**).* Yield = 49%; ^{1}H NMR (500 MHz, DMSO-d_6) δ 9.72 (s, 1H), 8.84 (d, J = 2.6 Hz, 1H), 8.77 (dd, J = 1.3, 2.9 Hz, 1H), 8.49 (dd, J = 2.5, 9.0 Hz, 1H), 8.31 (d, J = 9.1 Hz, 1H), 8.04 (dd, J = 1.2, 5.0 Hz, 1H), 7.83 (dd, J = 2.8, 5.1 Hz, 1H); HRMS (ESI-MS) calcd for $C_{12}H_8N_3O_2S^+$ *m/z* $(M + H)^+$ 258.0332, found: 258.0342.

*4.1.2.1.7. 2-(1-Methyl-1H-pyrazol-4-yl)-7-nitroquinoxaline (**17**).* Yield = 78%; ^{1}H NMR (400 MHz, DMSO-d_6) δ 9.47 (s, 1H), 8.74–8.67 (m, 2H), 8.42 (dd, J = 9.1, 2.6 Hz, 1H), 8.34 (s, 1H), 8.25 (d, J = 9.1 Hz, 1H), 3.97 (s, 3H); HRMS (ESI-MS) calcd for $C_{12}H_{10}N_5O_2^+$ *m/z* $(M + H)^+$ 256.0829, found: 256.0838.

*4.1.2.1.8. 2-(1-Methyl-1H-pyrrol-3-yl)-7-nitroquinoxaline (**17a**).* Yield = 48%; ^{1}H NMR (400 MHz, $CDCl_3$) δ 9.20 (s, 1H), 9.02 (d, J = 2.5 Hz, 1H), 8.40 (dd, J = 9.1, 2.5 Hz, 1H), 8.17 (d, J = 9.1 Hz, 1H), 7.73 (t, J = 2.0 Hz, 1H), 6.95 (dd, J = 2.9, 1.8 Hz, 1H), 6.80–6.77 (m, 1H), 3.82 (s, 3H); HRMS (ESI-MS) calcd for $C_{13}H_{11}N_4O_2^+$ *m/z* $(M + H)^+$ 255.0877, found: 255.0882.

*4.1.2.1.9. 6-Nitro-2-phenylquinoxaline (**23**).* Yield = 58%; ^{1}H NMR (400 MHz, DMSO-d_6) δ 9.83 (s, 1H), 8.94 (d, J = 2.5 Hz, 1H), 8.59 (dd, J = 9.2, 2.6 Hz, 1H), 8.44 (dd, J = 6.7, 2.9 Hz, 2H), 8.37 (d, J = 9.2 Hz, 1H), 7.66 (m, 3H); HRMS (ESI-MS) calcd for $C_{14}H_{10}N_3O_2^+$ *m/z* $(M + H)^+$ 252.0768, found: 252.0778.

*4.1.2.1.10. 6-Nitro-2-(thiophen-2-yl)quinoxaline (**24**).* Yield = 62%; ^{1}H NMR (500 MHz, CDCl3) δ 9.38 (s, 1H), 8.98 (d, J = 2.5 Hz, 1H), 8.53 (dd, J = 2.5, 9.2 Hz, 1H), 8.24 (d, J = 9.2 Hz, 1H), 8.04 (d, J = 3.7 Hz, 1H), 7.68 (dd, J = 1.2, 5.1 Hz, 1H), 7.27 (dd, J = 3.8, 5.0 Hz, 1H); HRMS (ESI-MS) calcd for $C_{12}H_8N_3O_2S^+$ *m/z* $(M + H)^+$ 258.0332, found: 258.0326.

*4.1.2.1.11. 6-Nitro-2-(thiophen-3-yl)quinoxaline (**25**).* Yield = 54%; ^{1}H NMR (500 MHz, $CDCl_3$) δ 9.38 (s, 1H), 8.98 (d, J = 2.5 Hz, 1H), 8.53 (dd, J = 2.5, 9.2 Hz, 1H), 8.24 (d, J = 9.2 Hz, 1H), 8.04 (d, J = 3.7 Hz, 1H), 7.68 (dd, J = 1.2, 5.1 Hz, 1H), 7.27 (dd, J = 3.8, 5.0 Hz, 1H); HRMS (ESI-MS) calcd for $C_{12}H_8N_3O_2S^+$ *m/z* $(M + H)^+$ 258.0332, found: *258.0342.*

*4.1.2.1.12. 2-(1-Methyl-1H-pyrazol-4-yl)-6-nitroquinoxaline (**26**).* ^{1}H NMR (400 MHz, DMSO-d_6) δ 9.49 (s, 1H), 8.82 (d, J = 2.4 Hz, 1H), 8.74 (s, 1H), 8.50 (dd, J = 9.2, 2.5 Hz, 1H), 8.37 (s, 1H), 8.16 (d, J = 9.2 Hz, 1H), 3.98 (s, 3H); HRMS (ESI-MS) calcd for $C_{12}H_{10}N_5O_2^+$ *m/z* $(M + H)^+$ 256.0829, found: 256.0839.

*4.1.2.1.13. 2-(4-bromophenyl)-N-(2,3-di(furan-2-yl)quinoxalin-6-yl)acetamide (**40**).* A mixture of Compound **7** (1 eq) and DIPEA (3 eq) was dissolved in DCM. To this mixture was added EDC (2 eq) and was stirred for 10 min at 0 °C followed by addition of 4-bromophenylacetic (3eq). The reaction mixture was further stirred for 8 h at room temperature and then extracted with EtOAc. The organic layer was washed with brine, dried over Na_2SO_4 and evaporated under reduced pressure. Then crude was purified on silica gel chromatography using hexane/EtOAc as eluting solvents to yield **40** as pure compound; Yield = 85%; ^{1}H NMR (500 MHz, Chloroform-*d*) δ 8.24 (d, J = 2.3 Hz, 1H), 8.04 (d, J = 9.1 Hz, 1H), 7.88 (dd, J = 9.1, 2.4 Hz, 1H), 7.75 (s, 1H), 7.60 (d, J = 1.7 Hz, 2H), 7.56–7.50 (m, 2H), 7.25 (s, 1H), 6.65 (dd, J = 14.8, 3.4 Hz, 2H), 6.55 (dd, J = 3.5, 1.8 Hz, 2H), 3.77 (s, 2H); HRMS (ESI-MS) calcd for $C_{24}H_{17}BrN_3O_3^+$ *m/z* $(M + H)^+$ 474.0448, found: 474.0155.

*4.1.2.1.14. 2-(4-bromophenyl)-N-(2,3-diphenylquinoxalin-6-yl) acetamide (**46**).* Same method as used for the synthesis of **40** starting from compound **10**; Yield = 90%; ^{1}H NMR (500 MHz, DMSO-d_6) δ 10.74 (s, 1H), 8.56 (d, J = 2.3 Hz, 1H), 8.10 (d, J = 9.0 Hz, 1H), 7.94 (dd, J = 9.0, 2.3 Hz, 1H), 7.55 (d, J = 8.1 Hz, 2H), 7.49–7.42 (m, 4H), 7.42–7.31 (m, 8H), 3.78 (s, 2H); HRMS (ESI-MS) calcd for $C_{24}H_{17}BrN_3O_3^+$ *m/z* $(M + H)^+$ 474.0448, found: 474.0452.

*4.1.2.1.15. 1-(3-bromophenyl)-3-(2,3-diphenylquinoxalin-6-yl) urea (**47**).* Yield = 72%; ^{1}H NMR (500 MHz, DMSO-d_6) δ 9.37 (s, 1H), 9.11 (s, 1H), 8.43–8.29 (m, 1H), 8.07 (d, J = 9.0 Hz, 1H), 7.90 (d, J = 1.8 Hz, 1H), 7.88–7.76 (m, 1H), 7.52–7.42 (m, 4H), 7.37 (dt, J = 8.3, 13.2 Hz, 7H), 7.28 (t, J = 8.0 Hz, 1H), 7.19 (d, J = 7.9 Hz, 1H); ^{13}C NMR (125 MHz, DMSO-d_6) δ 153.1, 152.3, 150.8, 141.4, 141.0, 138.9, 138.9, 136.8, 130.7, 129.6, 129.6, 129.2, 128.6, 128.4, 128.0, 128.0, 124.7, 123.7, 121.7, 120.7, 117.3, 113.4. HRMS (ESI-MS) calcd for $C_{27}H_{20}BrN_4O^+$ *m/z* $(M + H)^+$ 495.0815, found: 495.0817.

*4.1.2.1.16. 1-(2-bromophenyl)-3-(2,3-diphenylquinoxalin-6-yl) urea (**48**).* Yield = 69%; ^{1}H NMR (500 MHz, DMSO-d_6) δ 10.02 (s, 1H), 8.42 (d, J = 2.4 Hz, 1H), 8.36 (s, 1H), 8.10 (t, J = 8.2 Hz, 2H), 7.80 (dd, J = 2.5, 9.0 Hz, 1H), 7.65 (d, J = 8.0 Hz, 1H), 7.53–7.42 (m, 4H), 7.42–7.26 (m, 7H), 7.03 (t, J = 7.7 Hz, 1H); ^{13}C NMR (125 MHz, DMSO-d_6) δ 153.2, 152.1, 150.8, 141.5, 141.1, 138.9, 136.8, 136.7, 132.6, 129.7, 129.6, 129.4, 128.7, 128.5, 128.2, 128.0, 128.0, 124.6, 123.6, 122.6, 113.5, 113.3; HRMS (ESI-MS) calcd for $C_{27}H_{20}BrN_4O^+$ *m/z* $(M + H)^+$ 495.0815, found: 495.0821.

*4.1.2.1.17. 1-(2,3-Diphenylquinoxalin-6-yl)-3-(4-fluorophenyl) urea (**49**).* Yield = 64%; ^{1}H NMR (500 MHz, DMSO-d_6) δ 9.30 (s, 1H), 8.95 (s, 1H), 8.36 (d, J = 2.3 Hz, 1H), 8.06 (d, J = 9.0 Hz, 1H), 7.83 (dd, J = 2.4, 9.1 Hz, 1H), 7.53 (dd, J = 4.9, 8.8 Hz, 2H), 7.45 (dd, J = 7.0, 11.0 Hz, 4H), 7.35 (h, J = 6.7 Hz, 6H), 7.16 (t, J = 8.7 Hz, 2H); ^{13}C NMR (125 MHz, DMSO-d_6) δ 158.5, 156.6, 154.1, 153.1, 152.5, 150.7, 141.5, 141.4, 139.0, 139.0, 136.7, 135.7, 129.7, 129.6, 129.2, 128.7, 128.4, 128.0, 128.0, 123.7, 120.4, 120.3, 115.5, 115.4, 115.3, 115.2, 113.1; HRMS (ESI-MS) calcd for $C_{27}H_{20}FN_4O^+$ *m/z* $(M + H)^+$ 435.1616, found: 436.1623.

*4.1.2.1.18. 1-(4-chlorophenyl)-3-(2,3-diphenylquinoxalin-6-yl) urea (**50**).* Yield = 68%; ^{1}H NMR (500 MHz, DMSO-d_6) δ 9.34 (s, 1H), 9.06 (s, 1H), 8.36 (d, J = 2.3 Hz, 1H), 8.07 (d, J = 9.0 Hz, 1H), 7.84 (dd, J = 2.4, 9.1 Hz, 1H), 7.54 (d, J = 8.6 Hz, 2H), 7.51–7.42 (m, 4H), 7.36 (dt, J = 6.7, 9.7 Hz, 8H); ^{13}C NMR (125 MHz, DMSO-d_6) δ 153.1, 152.3, 150.7, 141.5, 141.2, 139.0, 138.9, 138.3, 136.8, 129.7, 129.6, 129.3, 128.7, 128.7, 128.5, 128.0, 128.0, 125.8, 123.7, 120.0, 113.3; HRMS (ESI-MS) calcd for $C_{27}H_{20}ClN_4O^+$ *m/z* $(M + H)^+$ 451.1320, found: 451.1327.

*4.1.2.1.19. 1-(2,3-Diphenylquinoxalin-6-yl)-3-(4-methoxyphenyl) urea (**51**).* Yield = 81%; ^{1}H NMR (500 MHz, DMSO-d_6) δ 9.23 (s, 1H), 8.72 (s, 1H), 8.36 (s, 1H), 8.05 (d, J = 9.0 Hz, 1H), 7.83 (d, J = 9.2 Hz, 1H), 7.50–7.32 (m, 12H), 6.91 (d, J = 8.4 Hz, 2H), 3.73 (s, 3H); ^{13}C NMR (125 MHz, DMSO-d_6) δ 154.8, 153.1, 152.6, 150.5, 141.5, 139.0, 136.7, 132.3, 129.7, 129.6 (3C), 129.2, 128.6, 128.4, 128.0, 128.0 (2C), 123.7, 120.4 (2C), 114.1 (2C), 112.8, 55.2; HRMS (ESI-MS) calcd for $C_{28}H_{23}N_4O_2^+$ *m/z* $(M + H)^+$ 447.1816, found: 447.1817.

*4.1.2.1.20. 1-(2,3-Diphenylquinoxalin-6-yl)-3-(4-(trifluoromethyl) phenyl)urea (**52**).* Yield = 83%; ^{1}H NMR (500 MHz, DMSO-d_6) δ 9.43 (s, 1H), 9.34 (s, 1H), 8.38 (s, 1H), 8.08 (d, J = 9.0 Hz, 1H), 7.85 (d, J = 9.1 Hz, 1H), 7.77–7.61 (m, 4H), 7.46 (dd, J = 7.3, 11.5 Hz, 4H), 7.36 (h, J = 6.9 Hz, 6H); ^{13}C NMR (125 MHz, DMSO-d_6) δ 153.2, 152.2, 150.9, 143.1, 141.4, 141.0, 138.9, 138.9, 136.9, 129.7, 129.6, 129.3, 128.7, 128.5, 128.0, 128.0, 126.1, 125.6, 123.7, 123.4, 122.0, 118.1, 117.8, 113.5, 67.0; HRMS (ESI-MS) calcd for $C_{28}H_{20}F_3N_4O^+$ *m/z* $(M + H)^+$ 485.1584, found: 485.1587.

*4.1.2.1.21. 1-(2,4-bis(trifluoromethyl)phenyl)-3-(2,3-diphenylquinoxalin-6-yl)urea (**53**).* Yield = 59%; ^{1}H NMR (500 MHz, DMSO-d_6) δ 9.61 (d, J = 8.9 Hz, 2H), 8.38 (d, J = 2.3 Hz, 1H), 8.19 (s, 2H), 8.07 (d, J = 9.0 Hz, 1H), 7.89 (dd, J = 2.3, 9.0 Hz, 1H), 7.67 (s, 1H), 7.53–7.42 (m, 4H), 7.42–7.24 (m, 6H); ^{13}C NMR (125 MHz, DMSO-d_6) δ 153.1, 152.4, 151.0, 141.5, 141.3, 140.7, 138.9, 136.9, 131.1, 130.9, 130.6, 130.3, 129.7, 129.6, 129.2, 128.7, 128.5, 128.0, 124.4, 123.9, 122.2, 118.3, 114.7, 114.1; HRMS (ESI-MS) calcd for $C_{29}H_{19}F_6N_4O^+$ *m/z* $(M + H)^+$ 553.1458, found: 553.1462.

*4.1.2.1.22. 1-(4-fluorophenyl)-3-(3-phenylquinoxalin-6-yl)urea (**54**).* Yield = 54%; ^{1}H NMR (500 MHz, DMSO-d_6) δ 9.39 (s, 1H), 9.27 (s, 1H), 8.94 (s, 1H), 8.36 (d, J = 2.3 Hz, 1H), 8.34–8.27 (m, 2H), 8.02 (d, J = 9.0 Hz, 1H), 7.78 (dd, J = 2.4, 9.0 Hz, 1H), 7.64–7.46 (m, 5H), 7.16 (t, J = 8.8 Hz, 2H); ^{13}C NMR (125 MHz, DMSO-d_6) δ 158.7, 156.8, 152.7, 151.3, 142.7, 141.7, 141.4, 137.6, 136.4, 135.8, 130.4, 129.4, 129.2,

127.5, 123.3, 120.5, 120.4, 115.6, 115.4, 113.8; HRMS (ESI-MS) calcd for $C_{21}H_{16}FN_4O^+$ *m/z* $(M + H)^+$ 359.1303, found: 359.1313.

4.1.2.1.23. 1-(4-chlorophenyl)-3-(3-phenylquinoxalin-6-yl)urea ***(55)***. Yield = 61%; ^{1}H NMR (500 MHz, DMSO-d_6) δ 9.40 (s, 1H), 9.32 (s, 1H), 9.06 (s, 1H), 8.36 (d, J = 2.4 Hz, 1H), 8.35–8.29 (m, 2H), 8.03 (d, J = 9.0 Hz, 1H), 7.79 (dd, J = 9.0, 2.4 Hz, 1H), 7.64–7.52 (m, 5H), 7.40–7.34 (m, 2H); ^{13}C NMR (125 MHz, $CDCl_3$) δ 152.6, 151.4, 142.7, 141.6, 138.6, 137.7, 136.5, 130.5, 129.5, 129.3, 129.0, 127.6, 126.0, 123.4, 120.3, 114.0; HRMS (ESI-MS) calcd for $C_{21}H_{16}ClN_4O^+$ *m/z* $(M + H)^+$ 375.1007, found: 375.1017.

4.1.2.1.24. 1-(4-bromophenyl)-3-(3-phenylquinoxalin-6-yl)urea ***(56)***. Yield = 83%; ^{1}H NMR (500 MHz, DMSO-d_6) δ 9.40 (s, 1H), 9.32 (s, 1H), 9.06 (s, 1H), 8.40–8.27 (m, 3H), 8.03 (d, J = 9.0 Hz, 1H), 7.79 (dd, J = 2.4, 9.1 Hz, 1H), 7.59 (dd, J = 7.1, 11.5 Hz, 3H), 7.50 (s, 4H); ^{13}C NMR (125 MHz, DMSO-d_6) δ 152.3, 151.1, 142.5, 141.3, 141.2, 138.8, 137.5, 136.2, 131.5, 131.5, 130.2, 129.2, 129.0, 127.3, 123.1, 120.4, 120.2, 113.8, 113.6; HRMS (ESI-MS) calcd for $C_{21}H_{16}BrN_4O^+$ *m/z* $(M + H)^+$ 419.0502, found: 419.0507.

4.1.2.1.25. 1-(3-bromophenyl)-3-(3-phenylquinoxalin-6-yl)urea ***(57)***. Yield = 63%; ^{1}H NMR (500 MHz, DMSO-d_6) δ 9.39 (d, J = 8.3 Hz, 2H), 9.13 (s, 1H), 8.39–8.27 (m, 3H), 8.03 (d, J = 9.0 Hz, 1H), 7.91 (t, J = 2.0 Hz, 1H), 7.79 (dd, J = 2.4, 9.0 Hz, 1H), 7.64–7.50 (m, 4H), 7.39 (dd, J = 1.9, 8.2 Hz, 1H), 7.28 (t, J = 8.0 Hz, 1H), 7.20 (dd, J = 1.8, 7.9 Hz, 1H); ^{13}C NMR (125 MHz, DMSO-d_6) δ 152.3, 151.1, 142.4, 141.3, 141.2, 141.0, 137.5, 136.2, 130.7, 130.3, 129.2, 129.1, 127.3, 124.7, 123.2, 121.7, 120.7, 117.3, 113.9; HRMS (ESI-MS) calcd for $C_{21}H_{16}BrN_4O^+$ *m/z* $(M + H)^+$ 419.0502, found: 419.0505.

4.1.2.1.26. 1-(2-bromophenyl)-3-(3-phenylquinoxalin-6-yl)urea ***(58)***. Yield = 64%; ^{1}H NMR (500 MHz, DMSO-d_6) δ 9.19 (s, 1H), 8.56 (s, 1H), 7.58 (d, J = 2.3 Hz, 1H), 7.53 (s, 1H), 7.50–7.45 (m, 2H), 7.27 (dd, J = 1.5, 8.3 Hz, 1H), 7.20 (d, J = 8.9 Hz, 1H), 6.90 (dd, J = 2.3, 9.1 Hz, 1H), 6.81 (dd, J = 1.3, 8.0 Hz, 1H), 6.74 (dq, J = 7.1, 13.9 Hz, 3H), 6.55 (t, J = 7.7 Hz, 1H), 6.18 (t, J = 7.5 Hz, 1H); ^{13}C NMR (125 MHz, DMSO-d_6) δ 152.1, 151.1, 142.5, 141.3, 141.2, 137.5, 136.7, 136.2, 132.5, 130.3, 129.4, 129.1, 128.1, 127.3, 124.5, 123.0, 122.6, 113.8, 113.5; HRMS (ESI-MS) calcd for $C_{21}H_{16}BrN_4O^+$ *m/z* $(M + H)^+$ 419.0502, found: 419.0507.

4.1.2.1.27. 1-(4-methoxyphenyl)-3-(3-phenylquinoxalin-6-yl)urea ***(59)***. Yield = 59%; ^{1}H NMR (500 MHz, DMSO-d_6) δ 9.38 (s, 1H), 9.21 (s, 1H), 8.71 (s, 1H), 8.35 (d, J = 2.3 Hz, 1H), 8.34–8.26 (m, 2H), 8.01 (d, J = 9.0 Hz, 1H), 7.77 (dd, J = 2.4, 9.0 Hz, 1H), 7.66–7.52 (m, 3H), 7.46–7.34 (m, 2H), 6.97–6.85 (m, 2H), 3.73 (s, 3H); ^{13}C NMR (125 MHz, $CDCl_3$) δ 155.0, 152.8, 151.4, 142.8, 142.0, 137.6, 136.5, 132.5, 130.5, 129.4, 129.3, 127.6, 123.4, 120.7, 114.3, 113.6, 55.4; HRMS (ESI-MS) calcd for $C_{22}H_{19}N_4O_2^+$ *m/z* $(M + H)^+$ 371.1503, found: 371.1509.

4.1.2.1.28. 1-(3-Phenylquinoxalin-6-yl)-3-(4-(trifluoromethyl) phenyl)urea ***(60)***. Yield = 53%; ^{1}H NMR (500 MHz, DMSO-d_6) δ 8.60 (s, 1H), 8.57 (s, 1H), 8.53 (s, 1H), 7.55 (d, J = 2.3 Hz, 1H), 7.52–7.45 (m, 2H), 7.20 (d, J = 9.0 Hz, 1H), 6.97 (dd, J = 2.4, 9.0 Hz, 1H), 6.89 (d, J = 8.6 Hz, 2H), 6.84 (d, J = 8.6 Hz, 2H), 6.79–6.68 (m, 3H); ^{13}C NMR (125 MHz, DMSO-d_6) δ 152.2, 151.1, 143.1, 142.4, 141.4, 141.1, 137.5, 136.2, 130.3, 129.3, 129.1, 127.3, 126.1, 123.4, 123.2, 118.1, 114.0; HRMS (ESI-MS) calcd for $C_{22}H_{16}F_3N_4O^+$ *m/z* $(M + H)^+$ 409.1271, found: 409.1277.

4.1.2.1.29. 1-(2,4-bis(trifluoromethyl)phenyl)-3-(3-phenylquinoxalin-6-yl)urea ***(61)***. Yield = 82%; ^{1}H NMR (500 MHz, DMSO-d_6) δ 9.64 (s, 1H), 9.61 (s, 1H), 9.43 (s, 1H), 8.40 (d, J = 2.3 Hz, 1H), 8.37–8.30 (m, 2H), 8.20 (s, 2H), 8.05 (d, J = 9.0 Hz, 1H), 7.85 (dd, J = 2.4, 9.0 Hz, 1H), 7.69 (s, 1H), 7.64–7.50 (m, 3H); ^{13}C NMR (125 MHz, DMSO-d_6) δ 152.4, 151.2, 142.5, 141.5, 137.6, 136.2, 130.3, 129.2, 129.1, 127.3, 123.3, 118.3, 114.6; HRMS (ESI-MS) calcd for $C_{23}H_{15}F_6N_4O^+$ *m/z* $(M + H)^+$ 477.1145, found: 477.1151.

4.1.2.1.30. 1-(4-fluorophenyl)-3-(2-phenylquinoxalin-6-yl)urea ***(62)***. Yield = 68%; ^{1}H NMR (500 MHz, DMSO-d_6) δ 9.48 (s, 1H), 9.28 (s, 1H), 8.93 (s, 1H), 8.35 (d, J = 2.3 Hz, 1H), 8.32–8.24 (m, 2H), 8.06 (d, J = 9.0 Hz, 1H), 7.83 (dd, J = 2.4, 9.2 Hz, 1H), 7.64–7.47 (m, 5H), 7.16 (t, J = 8.7 Hz, 2H). ^{13}C NMR (125 MHz, $CDCl_3$) δ 158.7, 156.8, 152.7, 149.0, 144.0, 142.3, 141.1, 137.8, 136.5, 135.8, 130.1, 129.8, 129.2, 127.2, 124.0, 120.6, 120.5, 115.6, 115.4, 113.6; HRMS (ESI-MS) calcd for $C_{21}H_{16}FN_4O^+$ *m/z* $(M + H)^+$ 359.1303, found: 359.1310.

4.1.2.1.31. 1-(4-chlorophenyl)-3-(2-phenylquinoxalin-6-yl)urea ***(63)***. Yield = 54%; ^{1}H NMR (500 MHz, DMSO-d_6) δ 9.49 (s, 1H), 9.32 (s, 1H), 9.04 (s, 1H), 8.35 (d, J = 2.3 Hz, 1H), 8.33–8.26 (m, 2H), 8.07 (d, J = 9.0 Hz, 1H), 7.83 (dd, J = 2.4, 9.1 Hz, 1H), 7.63–7.50 (m, 5H), 7.41–7.31 (m, 2H); ^{13}C NMR (125 MHz, $CDCl_3$) δ 152.3, 148.9, 143.8, 142.0, 140.8, 138.3, 137.7, 136.3, 129.9, 129.6, 129.0, 128.7, 127.0, 125.7, 123.8, 120.0, 113.5; HRMS (ESI-MS) calcd for $C_{21}H_{16}ClN_4O^+$ *m/z* $(M + H)^+$ 375.1007, found: 375.1014.

4.1.2.1.32. 1-(4-bromophenyl)-3-(2-phenylquinoxalin-6-yl)urea ***(64)***. Yield = 83%; ^{1}H NMR (500 MHz, DMSO-d_6) δ 9.49 (s, 1H), 9.34 (s, 1H), 9.06 (s, 1H), 8.35 (d, J = 2.3 Hz, 1H), 8.30 (dd, J = 1.7, 7.6 Hz, 2H), 8.06 (d, J = 9.0 Hz, 1H), 7.83 (dd, J = 2.4, 9.1 Hz, 1H), 7.63–7.53 (m, 3H), 7.50 (s, 4H); ^{13}C NMR (125 MHz, DMSO-d_6) δ 152.3, 148.9, 143.8, 142.0, 140.7, 138.8, 137.7, 136.3, 131.6, 129.9, 129.6, 129.0, 127.0, 123.8, 120.4, 113.6, 113.5; HRMS (ESI-MS) calcd for $C_{21}H_{16}BrN_4O^+$ *m/z* $(M + H)^+$ 419.0502, found: 419.0506.

4.1.2.1.33. 1-(3-bromophenyl)-3-(2-phenylquinoxalin-6-yl)urea ***(65)***. Yield = 64%; ^{1}H NMR (500 MHz, DMSO-d_6) δ 10.55 (s, 1H), 10.28 (s, 1H), 9.42 (s, 1H), 8.41 (d, J = 2.3 Hz, 1H), 8.25 (d, J = 7.4 Hz, 2H), 7.96–7.87 (m, 3H), 7.54 (dq, J = 13.5, 7.2 Hz, 4H), 7.20–7.07 (m, 2H); ^{13}C NMR (125 MHz, DMSO-d_6) δ 152.7, 148.5, 143.5, 142.1, 141.8, 141.5, 137.5, 136.4, 130.4, 129.8, 129.1, 129.0, 127.0, 124.2, 121.6, 120.6, 117.2, 113.4; HRMS (ESI-MS) calcd for $C_{21}H_{16}BrN_4O^+$ *m/z* $(M + H)^+$ 419.0502, found: 419.0503.

4.1.2.1.34. 1-(2-bromophenyl)-3-(2-phenylquinoxalin-6-yl)urea ***(66)***. Yield = 59%; ^{1}H NMR (500 MHz, DMSO-d_6) δ 10.08 (s, 1H), 9.48 (s, 1H), 8.50–8.36 (m, 2H), 8.29 (d, J = 7.5 Hz, 2H), 8.07 (t, J = 8.3 Hz, 2H), 7.91–7.77 (m, 1H), 7.64 (d, J = 8.0 Hz, 1H), 7.56 (dt, J = 7.4, 24.5 Hz, 3H), 7.38 (t, J = 7.8 Hz, 1H), 7.03 (t, J = 7.7 Hz, 1H); ^{13}C NMR (125 MHz, DMSO-d_6) δ 152.2, 148.9, 143.8, 142.1, 140.8, 137.7, 136.8, 136.3, 132.5, 129.9, 129.7, 129.1, 128.1, 127.0, 124.6, 123.7, 122.8, 113.8, 113.5; HRMS (ESI-MS) calcd for $C_{21}H_{16}BrN_4O^+$ *m/z* $(M + H)^+$ 419.0502, found: 419.0505.

4.1.2.1.35. 1-(4-methoxyphenyl)-3-(2-phenylquinoxalin-6-yl)urea ***(67)***. Yield = 51%; ^{1}H NMR (500 MHz, DMSO-d_6) δ 10.18 (s, 1H), 9.66 (s, 1H), 9.47 (s, 1H), 8.40 (m, 2H), 8.30 (d, J = 7.6 Hz, 2H), 8.04 (d, J = 8.0 Hz, 1H), 7.91 (dd, J = 8.0 Hz, 1H), 7.63–7.50 (m, 6H), 3.71 (s, 3H). ^{13}C NMR (126 MHz, $CDCl_3$) δ 154.7, 152.5, 148.7, 143.7, 142.1, 141.1, 137.5, 136.3, 132.2, 129.8, 129.6, 129.0, 127.0, 123.8, 120.4, 114.0, 113.1, 55.2; HRMS (ESI-MS) calcd for $C_{22}H_{19}N_4O_2^+$ *m/z* $(M + H)^+$ 371.1503, found: 375.1511.

4.1.2.1.36. 1-(2-Phenylquinoxalin-6-yl)-3-(4-(trifluoromethyl) phenyl)urea ***(68)***. Yield = 63%; ^{1}H NMR (500 MHz, DMSO-d_6) δ 9.50 (s, 1H), 9.43 (s, 1H), 9.34 (s, 1H), 8.37 (d, J = 1.9 Hz, 1H), 8.35–8.25 (m, 2H), 8.08 (d, J = 9.0 Hz, 1H), 7.92–7.80 (m, 2H), 7.73 (d, J = 8.5 Hz, 2H), 7.68 (d, J = 8.5 Hz, 2H), 7.64–7.48 (m, 3H); ^{13}C NMR (125 MHz, DMSO-d_6) δ 152.2, 149.0, 143.8, 143.1, 142.0, 140.5, 137.8, 136.2, 129.9, 129.7, 129.0, 127.0, 126.1, 123.9, 118.1, 113.8; HRMS (ESI-MS) calcd for $C_{22}H_{16}F_3N_4O^+$*m/z* $(M + H)^+$ 409.1271, found: 409.1279.

4.1.2.1.37. 1-(2,4-bis(trifluoromethyl)phenyl)-3-(2-phenylquinoxalin-6-yl)urea ***(69)***. Yield = 66%; ^{1}H NMR (500 MHz, DMSO-d_6) δ 10.62 (s, 1H), 10.48 (s, 1H), 9.38 (s, 1H), 8.31 (d, J = 2.1 Hz, 1H), 8.28–8.19 (m, 2H), 8.16 (s, 2H), 7.93–7.76 (m, 2H), 7.59–7.35 (m, 4H); ^{13}C NMR (125 MHz, DMSO-d_6) δ 152.5, 148.7, 143.5, 142.0, 141.9, 140.8, 137.6, 136.3, 130.6, 130.4, 130.1, 129.8, 129.2, 129.0, 127.0, 124.3, 124.0, 122.2, 117.9, 114.1, 114.0; HRMS (ESI-MS) calcd for $C_{23}H_{15}F_6N_4O^+$ *m/z* $(M + H)^+$ 477.1145, found: 477.1149.

4.1.2.1.38. 1-(4-bromophenyl)-3-(3-(thiophen-2-yl)quinoxalin-6-yl)urea ***(70)***. Yield = 81%; ^{1}H NMR (500 MHz, DMSO-d_6) δ 9.39 (s, 1H), 9.29 (s, 1H), 9.06 (s, 1H), 8.26 (d, J = 2.4 Hz, 1H), 8.20 (dd, J = 1.1, 3.8 Hz, 1H), 7.99 (d, J = 9.0 Hz, 1H), 7.86 (dd, J = 1.0, 5.0 Hz, 1H), 7.72 (dd, J = 2.4, 9.1 Hz, 1H), 7.50 (s, 4H), 7.30 (dd, J = 3.7, 5.0 Hz, 1H); HRMS (ESI-MS) calcd for $C_{19}H_{14}BrN_4OS$ + m/z $(M + H)^+$ 425.0066, found: 425.0066.

4.1.2.1.39. 1-(4-bromophenyl)-3-(2-(thiophen-2-yl)quinoxalin-6-yl)urea ***(71)***. Yield = 57%; ^{1}H NMR (500 MHz, DMSO-d_6) δ 9.48 (s, 1H), 9.30 (s, 1H), 9.05 (s, 1H), 8.31 (d, J = 2.3 Hz, 1H), 8.15 (d, J = 3.6 Hz, 1H), 7.97 (d, J = 9.0 Hz, 1H), 7.84–7.71 (m, 2H), 7.50 (s, 4H), 7.28 (dd, J = 3.7, 5.0 Hz, 1H); ^{13}C NMR (125 MHz, DMSO-d_6) δ 152.3, 145.3, 142.9, 142.0, 141.7, 140.5, 138.8, 137.4, 131.6, 130.1, 129.0, 128.8, 127.6, 123.9, 120.4, 113.9, 113.7; HRMS (ESI-MS) calcd for $C_{19}H_{14}BrN_4OS$ + m/z $(M + H)^+$ 425.0066, found: 425.0068.

4.1.2.1.40. 1-(4-bromophenyl)-3-(3-(thiophen-3-yl)quinoxalin-6-yl)urea ***(72)***. Yield = 52%; ^{1}H NMR (500 MHz, DMSO-d_6) δ 9.36 (s, 1H), 9.30 (s, 1H), 9.05 (s, 1H), 8.61 (dd, J = 1.3, 2.8 Hz, 1H), 8.33 (d, J = 2.4 Hz, 1H), 8.03–7.96 (m, 2H), 7.78 (dd, J = 2.9, 5.1 Hz, 1H), 7.73 (dd, J = 2.4, 9.0 Hz, 1H), 7.50 (s, 4H); ^{13}C NMR (125 MHz, DMSO-d_6) δ 151.8, 147.4, 142.0, 141.2, 140.7, 138.8, 138.3, 136.6, 131.1, 131.0, 128.7, 127.2, 126.4, 125.9, 122.1, 119.8, 113.1, 113.1; HRMS (ESI-MS) calcd for $C_{19}H_{14}BrN_4OS$ + m/z $(M + H)^+$ 425.0066, found: 425.0071.

4.1.2.1.41. 1-(4-bromophenyl)-3-(2-(thiophen-3-yl)quinoxalin-6-yl)urea ***(73)***. Yield = 59%; ^{1}H NMR (500 MHz, DMSO-d_6) δ 9.43 (s, 1H), 9.29 (s, 1H), 9.04 (s, 1H), 8.52 (d, J = 2.9 Hz, 1H), 8.30 (d, J = 2.3 Hz, 1H), 8.00 (d, J = 9.0 Hz, 1H), 7.95 (d, J = 5.0 Hz, 1H), 7.80 (dd, J = 2.4, 9.1 Hz, 1H), 7.76 (dd, J = 2.9, 5.1 Hz, 1H), 7.49 (s, 4H); ^{13}C NMR (125 MHz, DMSO-d_6) δ 152.3, 145.9, 144.3, 141.7, 140.4, 139.3, 138.8, 137.6, 131.6 (2C), 129.3, 127.7, 126.3, 126.1, 123.7, 120.4 (2C), 113.8, 113.7; HRMS (ESI-MS) calcd for $C_{19}H_{14}BrN_4OS$ + m/z $(M + H)^+$ 425.0066, found: 425.0074.

4.1.2.1.42. 1-(4-bromophenyl)-3-(2-(1-methyl-1H-pyrazol-3-yl) quinoxalin-6-yl)urea ***(74)***. Yield = 80%; ^{1}H NMR (500 MHz, DMSO-d_6) δ 9.35 (s, 1H), 9.30 (s, 1H), 9.06 (s, 1H), 8.34 (d, J = 2.3 Hz, 1H), 8.05 (d, J = 9.0 Hz, 1H), 7.85 (dd, J = 2.4, 9.1 Hz, 1H), 7.61 (d, J = 2.0 Hz, 1H), 7.50 (s, 4H), 7.19 (d, J = 2.0 Hz, 1H), 4.30 (s, 3H); ^{13}C NMR (125 MHz, DMSO-d_6) δ 151.7, 144.7, 141.9, 140.9, 140.6, 138.2, 137.6, 137.5, 136.2, 131.1, 129.0, 123.4, 119.9, 113.2, 113.1, 107.4; HRMS (ESI-MS) calcd for $C_{19}H_{16}BrN_6O^+$ m/z $(M + H)^+$ 423.0563, found: 423.0571.

4.1.2.1.43. 1-(4-fluorophenyl)-3-(3-(1-methyl-1H-pyrazol-4-yl) quinoxalin-6-yl)urea ***(75)***. Yield = 61%; ^{1}H NMR (500 MHz, DMSO-d_6) δ 9.20 (s, 1H), 9.12 (s, 1H), 8.91 (s, 1H), 8.62 (s, 1H), 8.34–8.18 (m, 2H), 7.94 (d, J = 9.0 Hz, 1H), 7.68 (dd, J = 9.0, 2.3 Hz, 1H), 7.61–7.46 (m, 2H), 7.17 (t, J = 8.7 Hz, 2H), 3.96 (s, 3H) ppm; ^{13}C NMR (100 MHz, $CDCl_3$) δ 151.8, 144.2, 142.1, 141.2, 141.0, 138.2, 137.6, 137.4, 136.2, 131.1 (2C), 128.8, 122.9, 120.0 (2C), 113.2, 113.1, 107.9, 38.5; HRMS (ESI-MS) calcd for $C_{19}H_{15}FN_6O^+$ m/z $(M + H)^+$ 362.1291, found: 362.1299.

4.1.2.1.44. 1-(3-(1-methyl-1H-pyrazol-4-yl)quinoxalin-6-yl)-3-(p-tolyl)urea ***(76)***. Yield = 70%; ^{1}H NMR (500 MHz, $CDCl_3$) δ 9.16 (s, 1H), 9.11 (s, 1H), 8.76 (s, 1H), 8.62 (s, 1H), 8.27 (s, 1H), 8.24 (d, 1H, J = 2.0 Hz), 7.93 (d, 1H, J = 9.0 Hz), 7.66 (dd, 1H, J = 9.0, 2.0 Hz), 7.40 (d, 2H, J = 8.5 Hz), 7.13 (d, 2H, J = 8.5 Hz), 3.96 (s, 3H), 2.27 (s, 3H); ^{13}C NMR (100 MHz, $CDCl_3$) δ 151.9, 166.8, 142.2, 140.9, 140.7, 137.4, 136.3, 136.1, 130.6, 130.4, 128.7 (2C), 121.3, 119.7, 118.0 (2C), 117.7, 112.5, 38.5, 19.8; HRMS (ESI-MS) calcd for $C_{20}H_{19}N_6O$ + m/z $(M + H)^+$ 358.1542, found: 358.1551.

4.1.2.1.45. 1-(3-methoxyphenyl)-3-(3-(1-methyl-1H-pyrazol-4-yl) quinoxalin-6-yl)urea ***(77)***. Yield = 61%; ^{1}H NMR (400 MHz, DMSO-d_6) δ 9.17 (s, 1H), 9.10 (s, 1H), 8.87 (s, 1H), 8.60 (s, 1H), 8.28–8.21 (m, 2H), 7.92 (d, J = 9.0 Hz, 1H), 7.65 (dd, J = 9.0, 2.4 Hz, 1H), 7.26–7.16 (m, 2H), 6.98 (dd, J = 7.8, 2.0 Hz, 1H), 6.59 (dd, J = 8.2, 2.5 Hz, 1H), 3.94 (s, 3H), 3.75 (s, 3H); ^{13}C NMR (125 MHz, DMSO-d_6) δ 159.77, 152.41, 147.36, 142.77, 141.40, 141.28, 140.61, 138.01, 136.72, 130.98, 129.69, 129.30, 121.89, 120.28, 113.21, 110.82, 107.70, 104.29, 55.01, 41.39; HRMS (ESI-MS) calcd for $C_{20}H_{19}N_6O_2^+$ m/z $(M + H)^+$ 375.1564, found: 375.1564.

4.1.2.1.46. 1-(3-(1-methyl-1H-pyrazol-4-yl)quinoxalin-6-yl)-3-(3-(trifluoromethoxy)phenyl)urea ***(78)***. Yield = 55%; ^{1}H NMR (500 MHz, DMSO-d_6) δ 9.41 (s, 1H), 9.20 (s, 1H), 9.13 (d, J = 7.3 Hz, 1H), 8.62 (d, J = 5.6 Hz, 1H), 8.30–8.23 (m, 2H), 7.96 (dd, J = 15.0, 9.0 Hz, 1H), 7.74 (dd, J = 5.7, 3.1 Hz, 1H), 7.68 (dd, J = 9.2, 2.4 Hz, 1H), 7.47–7.29 (m, 2H), 6.98 (t, J = 9.6 Hz, 1H), 3.95 (d, J = 4.9 Hz, 3H); ^{13}C NMR (125 MHz, DMSO-d_6) δ 152.84, 149.21, 147.85, 143.15, 141.99, 141.71, 141.47, 138.45, 137.25, 131.43, 130.95, 129.82, 129.75, 122.34, 120.69, 117.54, 114.51, 113.99, 110.89, 40.26. MS calcd for $C_{20}H_{15}F_3N_6O_2$ m/z 428.12, found: 429.09 (M+1).

4.1.2.1.47. 1-(3-(1-methyl-1H-pyrazol-4-yl)quinoxalin-6-yl)-3-(3-(trifluoromethyl)phenyl)urea ***(79)***. Yield = 71%; ^{1}H NMR (500 MHz, DMSO-d_6) δ 9.44 (s, 1H), 9.36 (s, 1H), 9.12 (s, 1H), 8.61 (s, 1H), 8.29–8.24 (m, 2H), 8.06 (d, J = 2.5 Hz, 1H), 7.94 (d, J = 9.0 Hz, 1H), 7.71 (dd, J = 9.0, 2.3 Hz, 1H), 7.65 (d, J = 8.2 Hz, 1H), 7.55 (t, J = 8.0 Hz, 1H), 7.35 (d, J = 7.7 Hz, 1H), 3.95 (s, 3H); ^{13}C NMR (125 MHz, DMSO-d_6) δ 152.95, 147.81, 143.12, 141.99, 141.45, 140.74, 138.44, 137.24, 131.40, 130.48, 129.73, 122.61, 122.40, 120.67, 114.88, 114.06, 79.59, 41.80; MS calcd for $C_{20}H_{15}F_3N_6O$ m/z 412.13, found: 413.17 (M+1).

4.1.2.1.48. 1-(3-Chloro-4-fluorophenyl)-3-(3-(1-methyl-1H-pyrazol-4-yl)quinoxalin-6-yl)urea ***(80)***. Yield = 72%; ^{1}H NMR (500 MHz, DMSO-d_6) δ 9.44 (s, 1H), 9.24 (s, 1H), 9.12 (s, 1H), 8.61 (s, 1H), 8.28–8.22 (m, 2H), 7.93 (d, J = 9.0 Hz, 1H), 7.85 (dd, J = 6.8, 2.4 Hz, 1H), 7.70 (dd, J = 9.0, 2.4 Hz, 1H), 7.43–7.30 (m, 2H), 3.95 (s, 3H); ^{13}C NMR (125 MHz, DMSO-d_6) δ 153.50, 152.46, 151.58, 147.32, 142.67, 141.45, 137.96, 136.78, 130.92, 129.24, 121.85, 120.22, 119.82, 118.84, 117.02, 116.94, 116.84, 116.77, 113.45, 42.10; HRMS (ESI-MS) calcd for $C_{19}H_{15}ClFN_6O^+$ m/z $(M + H)^+$ 397.0974, found: 397.0979.

4.1.2.1.49. 1-(4-Fluoro-3-methylphenyl)-3-(3-(1-methyl-1H-pyrazol-4-yl)quinoxalin-6-yl)urea ***(81)***. Yield = 57%; ^{1}H NMR (500 MHz, DMSO-d_6) δ 9.20 (s, 1H), 9.11 (s, 1H), 8.83 (s, 1H), 8.60 (s, 1H), 8.25 (d, J = 13.3 Hz, 2H), 7.92 (d, J = 9.0 Hz, 1H), 7.66 (d, J = 9.1 Hz, 1H), 7.44–7.38 (m, 1H), 7.34–7.29 (m, 1H), 7.08 (t, J = 9.1 Hz, 1H), 3.95 (s, 3H), 2.24 (s, 3H); ^{13}C NMR (125 MHz, DMSO-d_6) δ 157.74, 155.84, 153.10, 147.87, 143.30, 141.89, 138.53, 137.22, 135.87, 131.49, 129.80, 124.97, 122.41, 122.15, 120.79, 118.35, 115.66, 113.72, 39.51, 14.98; MS calcd for $C_{20}H_{17}FN_6O$ m/z 376.14, found: 377.10 (M+1).

4.1.2.1.50. 1-(4-Fluoro-3-methoxyphenyl)-3-(3-(1-methyl-1H-pyrazol-4-yl)quinoxalin-6-yl)urea ***(82)***. Yield = 65%; ^{1}H NMR (500 MHz, DMSO-d_6) δ 9.24 (s, 1H), 9.11 (s, 1H), 8.96 (s, 1H), 8.61 (s, 1H), 8.31–8.24 (m, 2H), 7.93 (d, J = 9.0 Hz, 1H), 7.67 (dd, J = 9.0, 2.4 Hz, 1H), 7.46 (dd, J = 8.0, 2.5 Hz, 1H), 7.14 (dd, J = 11.4, 8.7 Hz, 1H), 6.94 (ddd, J = 8.8, 3.7, 2.5 Hz, 1H), 3.95 (s, 3H), 3.84 (s, 2H); ^{13}C NMR (125 MHz, DMSO-d_6) δ 152.24, 147.04, 146.73, 145.83, 142.45, 141.10, 137.71, 136.43, 135.94, 135.91, 130.68, 128.97, 121.58, 119.97, 115.53, 112.95, 110.00, 104.44, 55.55, 40.20; HRMS (ESI-MS) calcd for $C_{20}H_{18}FN_6O_2^+$ m/z $(M + H)^+$ 393.1470, found: 393.1482.

4.1.2.1.51. 1-(4-Fluoro-3-(trifluoromethoxy)phenyl)-3-(3-(1-methyl-1H-pyrazol-4-yl)quinoxalin-6-yl)urea ***(83)***.
Yield = 60%; ^{1}H NMR (400 MHz, DMSO-d_6) δ 9.32 (s, 1H), 9.20 (s, 1H), 9.12 (s, 1H), 8.61 (s, 1H), 8.29–8.21 (m, 2H), 7.97–7.86 (m, 2H), 7.69 (dd, J = 9.0, 2.4 Hz, 1H), 7.46 (t, J = 9.6 Hz, 1H), 7.39 (ddd, J = 9.1, 4.2, 2.6 Hz, 1H), 3.95 (s, 3H); ^{13}C NMR (125 MHz, DMSO-d_6) δ 153.00, 138.59, 137.45, 131.62, 127.54, 124.95, 123.03, 120.08, 119.96, 119.90, 117.27, 117.09, 114.24, 108.03; MS calcd for $C_{20}H_{14}F_4N_6O_2$ m/z 446.11, found: 447.02 (M+1).

4.1.2.1.52. 1-(4-Fluoro-3-(trifluoromethyl)phenyl)-3-(3-(1-methyl-1H-pyrazol-4-yl)quinoxalin-6-yl)urea ***(84)***.
Yield = 64%; ^{1}H NMR (600 MHz, DMSO-d_6) δ 9.63 (s, 1H), 9.11 (s,

1H), 9.01 (s, 1H), 8.60 (s, 1H), 8.46 (m, 1H), 8.27 (d, J = 2.9 Hz, 1H), 8.26 (s, 1H), 7.94 (d, J = 8.9 Hz, 1H), 7.62 (dd, J = 9.0, 2.3 Hz, 1H), 7.41–7.37 (m, 2H), 4.01–3.82 (s, 3H); ^{13}C (125 MHz, DMSO-d_6) δ 151.97, 149.89, 148.23, 147.39, 142.66, 141.61, 140.64, 137.98, 136.82, 130.97, 129.41, 128.67, 128.61, 125.36, 125.01, 124.98, 123.56, 121.76, 121.64, 120.17, 119.95, 119.45, 116.83, 116.76, 116.61, 116.54, 113.43, 38.89; ^{19}F NMR (564 MHz, DMSO-d_6) δ −119.00 (3F), −60.68 (1F); HRMS (ESI-MS) calcd for $C_{20}H_{15}F_4N_6O^+$ m/z (M + H)$^+$ 431.1238, found: 431.1240.

4.1.2.1.53. 3-Bromo-6-nitroquinoline ***(32)***. 4-nitroaniline (5.0 g, 36.2 mmol) in acetic acid (35 mL) was treated with 2,2,3 tribromopropanal (11.7 g, 39.8 mmol) and the mixture was heated at 110 °C for 2 h. AcOH was evaporated in vacuum followed by extraction of crude with ethyl acetate and water. Organic layer was washed with sat. $NaHCO_3$ and brine, respectively and dried over Na_2SO_4. Crude product was purified by column chromatography using ethyl acetate and hexane as eluting solvents; Yield = 38.2% (3.5 g); ^{1}H NMR (400 MHz, DMSO-d_6) δ 9.23 (dt, J = 17.1, 8.6 Hz, 1H), 9.14 (d, J = 2.4 Hz, 1H), 8.89–8.73 (m, 2H), 7.86 (dd, J = 8.3, 4.2 Hz, 1H); HRMS Calculated for $C_9H_6BrN_2O_2$+ m/z 252.9607, found mass = 252.9611.

4.1.2.1.54. 3-(2-Methyl-1H-2l4-pyrazol-4-yl)-6-nitroquinoline ***(33)***. Compound **32** (250 mg, 0.987 mmol), Na_2CO_3 (209.4 mg, 1.97 mmol), DMF (3 mL), Dioxane (3 mL) and water (0.2 mL) were mixed together in a round bottom flask. The mixture was sonicated and degassed for 5 min by passing nitrogen through it. Degassing was followed by addition of $Pd(Ph_3)_4$ (57.0 mg, 0.04 mmol) and 1-Methylpyrazole-4-boronic acid pinacol ester (246.6 mg, 1.185 mmol). The reaction mixture was stirred under inert atmosphere at 100 °C overnight and quenched by addition of water to the reaction mixture. Precipitates formed were filtered and triturated in THF and hexane; Yield = 47.8% (120 mg); ^{1}H NMR (400 MHz, $CDCl_3$) δ 9.15 (dd, J = 4.1, 1.8 Hz, 1H), 8.65 (dd, J = 12.2, 2.5 Hz, 2H), 8.56 (s, 1H), 8.38 (dd, J = 8.3, 1.7 Hz, 1H), 8.23 (s, 1H), 7.62 (dd, J = 8.3, 4.2 Hz, 1H), 4.07 (s, 3H); ^{13}C NMR (100 MHz, $CDCl_3$) δ 152.6, 147.1, 139.3, 138.4, 134.2, 132.0, 122.7, 121.8, 119.5, 39.2; HRMS Calculated for $C_{14}H_{13}N_3O_2^+$ m/z 255.1002, found mass = 255.0891.

4.1.2.1.55. 3-(1-Methyl-1H-pyrazol-4-yl)quinolin-6-amine ***(34)***. Compound **34** was synthesized according to Method B; Yield = Quantitative; ^{1}H NMR (400 MHz, DMSO-d_6) δ 8.59–8.53 (m, 1H), 8.50 (s, 1H), 7.99 (s, 1H), 7.94 (d, J = 8.3 Hz, 1H), 7.42 (d, J = 2.4 Hz, 1H), 7.30 (dd, J = 8.3, 4.1 Hz, 1H), 6.70 (d, J = 2.3 Hz, 1H), 5.51 (s, 2H), 3.93 (s, 3H); HRMS Calculated for $C_{13}H_{13}N_4^+$ m/z 225.1135, found mass = 225.1208.

4.1.2.1.56. 1-(3-Bromo-4-fluorophenyl)-3-(3-(1-methyl-1H-pyrazol-4-yl)quinolin-6-yl)urea ***(85)***. Compound **86** was synthesized according to Method D; Yield = 32%; ^{1}H NMR (400 MHz, $CDCl_3$) δ 8.77 (d, J = 2.1 Hz, 2H), 8.72 (s, 1H), 8.34 (s, 1H), 8.07–7.90 (m, 3H), 7.76 (dd, J = 6.0, 2.4 Hz, 1H), 7.73 (d, J = 2.0 Hz, 1H), 7.36 (m, 1H), 7.33–7.21 (m, 1H), 6.96 (t, J = 8.5 Hz, 1H), 3.95 (s, 3H); ^{13}C NMR (100 MHz, CDCl3) δ 153.2, 147.5, 141.6, 138.7, 137.0, 136.3, 136.0, 131.7, 131.6, 129.7, 123.7, 121.3, 120.9, 119.6, 118.9, 116.3116.1, 113.2, 108.8, 108.6, 46.3; HRMS (ESI-MS) calcd for $C_{20}H_{16}BrFN_5O^+$ m/z (M + H)$^+$ 440.0517, found: 440.0511.

4.1.2.1.57. 1-(3-Bromo-4-fluorophenyl)-3-(3-(1-methyl-1H-pyrrol-3-yl)quinoxalin-6-yl)urea ***(86)***. Yield = 65%; ^{1}H NMR (400 MHz, DMSO-d_6) δ 9.27 (s, 1H), 9.09 (s, 1H), 9.06 (s, 1H), 8.18 (d, J = 2.3 Hz, 1H), 7.98 (dd, J = 6.3, 2.6 Hz, 1H), 7.89 (d, J = 9.0 Hz, 1H), 7.78 (t, J = 2.0 Hz, 1H), 7.63 (dd, J = 9.0, 2.4 Hz, 1H), 7.42 (ddd, J = 9.0, 4.5, 2.7 Hz, 1H), 7.34 (t, J = 8.8 Hz, 1H), 6.90 (t, J = 2.5 Hz, 1H), 6.84 (t, J = 2.0 Hz, 1H), 3.73 (s, 3H); ^{13}C NMR (100 MHz, DMSO-d_6) δ 158.21, 157.98, 154.38, 152.79, 152.40, 149.32, 140.80, 136.96, 136.26, 129.09, 124.12, 123.77, 122.55, 121.35, 120.93, 119.35, 116.77, 116.62, 113.53, 107.24, 36.15; HRMS (ESI-MS) calcd for $C_{20}H_{16}BrFN_5O^+$ m/z (M + H)$^+$ 440.0517, found: 440.0518.

4.1.2.1.58. 1-(benzo[d] [1,3]dioxol-5-yl)-3-(3-(1-methyl-1H-pyrazol-4-yl)quinoxalin-6-yl)urea ***(87)***. Yield = 70%; ^{1}H NMR (500 MHz, DMSO-d_6) δ 9.13 (d, J = 26.8 Hz, 2H), 8.77 (s, 1H), 8.60 (s, 1H), 8.33–8.13 (m, 2H), 7.92 (d, J = 9.0 Hz, 1H), 7.65 (dd, J = 8.9, 2.4 Hz, 1H), 7.25 (d, J = 2.1 Hz, 1H), 6.93–6.80 (m, 2H), 5.97 (d, J = 16.7 Hz, 2H), 3.95 (s, 3H); ^{13}C NMR (125 MHz, DMSO-d_6) δ 152.99, 147.75, 147.73, 143.21, 142.84, 141.85, 138.42, 137.09, 134.14, 131.39, 129.69, 122.29, 120.70, 113.50, 111.89, 108.64, 101.67, 101.37, 40.53, 39.36; MS calculated for $C_{20}H_{16}N_6O_3$ m/z 388.13, found: 389.15 (M+1).

4.1.2.1.59. 1-(2,3-dihydrobenzo[b] [1,4]dioxin-6-yl)-3-(3-(1-methyl-1H-pyrazol-4-yl)quinoxalin-6-yl)urea ***(88)***. Yield = 61%; ^{1}H NMR (500 MHz, DMSO-d_6) δ 9.12 (d, J = 15.1 Hz, 2H), 8.69 (s, 1H), 8.61 (s, 1H), 8.31–8.14 (m, 2H), 7.92 (d, J = 9.0 Hz, 1H), 7.65 (dd, J = 9.0, 2.4 Hz, 1H), 7.14 (d, J = 2.5 Hz, 1H), 6.94–6.70 (m, 2H), 4.37–4.14 (m, 4H), 3.95 (s, 3H); ^{13}C NMR (125 MHz, DMSO-d_6) δ 152.91, 147.75, 143.60, 143.22, 141.89, 141.71, 139.20, 138.41, 137.08, 133.41, 131.38, 129.68, 122.28, 120.71, 117.38, 113.42, 112.40, 108.27, 64.71, 64.37, 40.38; MS calculated for $C_{21}H_{18}N_6O_3$ m/z 402.14, found: 403.13 (M+1).

4.1.2.1.60. 1-(benzo[b]thiophen-4-yl)-3-(3-(1-methyl-1H-pyrazol-4-yl)quinoxalin-6-yl)urea ***(89)***. Yield = 52%; ^{1}H NMR (500 MHz, DMSO-d_6) δ 9.28 (s, 1H), 9.11 (s, 1H), 9.02 (s, 1H), 8.61 (s, 1H), 8.27 (d, J = 2.0 Hz, 2H), 8.15 (d, J = 2.0 Hz, 1H), 7.93 (t, J = 9.0 Hz, 2H), 7.75 (d, J = 5.4 Hz, 1H), 7.70 (dd, J = 9.0, 2.4 Hz, 1H), 7.46–7.39 (m, 2H), 3.95 (s, 3H); ^{13}C NMR (125 MHz, DMSO-d_6) δ 152.69, 147.34, 142.78, 141.47, 141.38, 140.15, 138.04, 136.72, 136.35, 133.14, 131.00, 129.31, 128.25, 124.05, 122.79, 121.93, 120.27, 117.13, 113.16, 112.76, 41.40; MS calculated for $C_{21}H_{16}N_6OS$ m/z 400.11, found: 401.02 (M+1).

4.1.2.1.61. 1-(2,3-Dihydro-1H-inden-4-yl)-3-(3-(1-methyl-1H-pyrazol-4-yl)quinoxalin-6-yl)urea ***(90)***. Yield = 56%; ^{1}H NMR (500 MHz, DMSO-d_6) δ 9.16 (s, 1H), 9.10 (s, 1H), 8.74 (s, 1H), 8.60 (s, 1H), 8.28–8.21 (m, 2H), 7.92 (d, J = 8.9 Hz, 1H), 7.66 (dd, J = 9.0, 2.4 Hz, 1H), 7.42 (d, J = 1.9 Hz, 1H), 7.20 (dd, J = 8.1, 2.1 Hz, 1H), 7.15 (d, J = 8.1 Hz, 1H), 3.95 (s, 3H), 2.83 (dt, J = 22.5, 7.4 Hz, 4H), 2.54 (s, 2H), 2.01 (p, J = 7.4 Hz, 2H); ^{13}C NMR (125 MHz, DMSO-d_6) δ 152.45, 147.25, 144.27, 142.74, 141.44, 141.21, 137.92, 137.48, 137.41, 136.59, 130.88, 129.19, 124.24, 121.75, 120.22, 116.75, 114.78, 112.92, 40.43, 32.55, 31.70, 25.21; MS calculated for $C_{22}H_{20}N_6O$ m/z 384.17, found: 385.13 (M+1).

4.1.2.1.62. 1-(2,3-Dihydrobenzofuran-4-yl)-3-(3-(1-methyl-1H-pyrazol-4-yl)quinoxalin-6-yl)urea ***(91)***. Yield = 66%; ^{1}H NMR (400 MHz, DMSO-d_6) δ 9.11 (d, J = 14.7 Hz, 2H), 8.62 (d, J = 13.3 Hz, 2H), 8.30–8.18 (m, 2H), 7.91 (d, J = 9.0 Hz, 1H), 7.66 (dd, J = 9.0, 2.4 Hz, 1H), 7.41 (d, J = 2.2 Hz, 1H), 7.13 (dd, J = 8.5, 2.3 Hz, 1H), 6.71 (d, J = 8.5 Hz, 1H), 4.50 (t, J = 8.6 Hz, 2H), 3.95 (s, 3H), 3.18 (t, J = 8.6 Hz, 2H); ^{13}C NMR (125 MHz, DMSO-d_6) δ 155.71, 153.15, 147.69, 143.19, 142.09, 141.64, 138.42, 137.03, 132.56, 131.38, 129.66, 128.01, 122.28, 120.68, 119.36, 117.33, 113.27, 109.06, 71.29, 40.37, 29.92; MS calculated for $C_{21}H_{18}N_6O_2$ m/z 386.15, found: 387.07 (M+1).

4.2. Biology

4.2.1. κB luciferase reporter assay

The following modifications were made to the previously reported method [16]. Cells were pre-incubated with compounds for 30 min, which was followed by a 6 h TNFα stimulation.

4.2.2. Caspase 3/7 assay

MiaPaCa2 cells (2.5×10^4) were plated in 96-well white walled clear bottom plate and allowed to attach overnight. DMSO solutions of the inhibitors were added (final concentration of DMSO 0.1%)

and incubated for 24 h. 21 h post drug addition, alamarBlue® (Biorad, BUF012B) was added at a volume of 1/10 total volume per well (10 μL) and cells were allowed to incubate for 3 h. The plate was then read for fluorescence at 560ex/590em on a Spectrmax m5e. The plate was then allowed to equilibrate to room temperature for 15 min. 100 μL of Caspase-Glo (Promega G8093) reagent was added and 2 h later the plate was read for luminescence at 1000 ms. Values were calculated by: ([Luminescence*100]/Fluorescence)/$DMSO_{avg}$ [60].

4.2.3. Immunoblotting

T3M4 cells were treated with analog **84** at indicated doses (0.5, 1.0, 2.0 and 5.0 μM for 6 h) and the indicated time points, (5 μM at 0.5, 3.0, 6.0, 12 and 24 h) and harvested. Equal amounts of protein (40 μg) were separated on 4–20% gradient SDS-PAGE gels (Bio rad, USA) and transferred to 0.45 μm PVDF membranes (Millipore, USA). After blocking in 5% nonfat skim milk powder for 1 h, the membranes were probed with the following primary antibodies p-IKKβ, IKKβ and β-actin (Cell Signaling Technology, USA) overnight at 4 °C and secondary antibody (Horse anti-mouse and Goat anti-rabbit, Cell Signaling Technology, USA) at room temperature for 1 h. Membranes were visualized with chemiluminescent detection kits (Bio rad, USA).

4.2.4. Live/dead cell assay

MiaPaCa2 cells were treated with 5 and 10 μM of analog **84** for 24 h and subjected to live/dead cell assay as per the manufacturer's instruction (Invitrogen, USA). Briefly, vehicle and compound **84** treated cells were washed with 1x PBS. 20 μl ethidium homodimer-1 (EthD-1, 2 mM) was dissolved in 10 mL PBS. To this solution, 5 μl of calcein acetoxymethyl ester (calcein-AM, 4 mM) was added. 500 μl of this mixture was added to the well and incubated for 30 min. The numbers of live and dead cells were detected with Nikon fluorescent microscopy (Nikon, Japan). The ratio of dead cells to total cells was calculated for quantitative comparisons using ImageJ (NIH, USA) software.

4.2.5. Colony formation assay

MiaPaCa2 cells (1.0×10^3) were seeded in 6-well plates. Cells were treated with 5 μM of analog 84 for 24 h. Next day cells were washed with 1x PBS and allowed to grow for 8–10 days, with a medium change every 3 days. The vehicle and compound 84 treated cells were fixed with 4% paraformaldehyde for 15 min, washed and stained with 0.5% crystal violet for 2 h at room temperature. The colony number was determined in triplicate after capturing the image in 10x bright field microscope.

4.2.6. Cell scratch assay

MiaPaCa2 cells were seeded in a 6-well plate. The next day media was discarded, scratched with 200 μl pipette tips, washed with 1x PBS. Scratched cells were treated with 5 μM of analog **84**. The gap generated by the pipette tip was examined and captured by a bright-field microscope (Nikon, Japan) at 0, 24 and 48 h. The result was analyzed using ImageJ (NIH, USA) software. The percentage of gap closure was calculated for quantitative comparisons.

4.2.7. Growth inhibition assay

We followed the method previously reported by us [61]. Concentrations (20, 10, 5, 2.5, 1.25 and 0,625 μM) of analog **84** used in the study to derive the reported IC_{50} values.

4.2.8. Pharmacokinetic studies

CD1 mice were orally administered 20 mg/kg of 13–197 or **84** in DMSO:PEG400:H_2O = 1:4:5 or intravenously administered 10 mg/kg of **84** in DMSO:PEG400:H_2O = 1:5:4. At following time points (0.083, 0.25, 0.5, 1, 2, 4, 8, 24 h) mice were sacrificed and the plasma was subjected to LC/MS/MS (AB Sciex Triple Quad 5500) and the compound levels determined using an internal standard method (Carbamazepine). The PK parameters were calculated using non-compartmental approach with PhoenixTM WinNonlin®, version 8.3 (Pharsight, CA).

4.2.9. Pancreatic tumor model

To assess *in vivo* efficacy of analog **84**, MiaPaCa2 cells (2.5×10^6 cells and Matrigel, 2:1 ratio) were subcutaneously implanted in left flank of athymic nude mice (Crl: NU-Foxn1nu, Charles River laboratories, USA). After 20 days of implantation, mice were randomized and grouped into the following treatment groups: Wehicle (100 μl daily orally), analog **84** (40 mg/kg body weight daily orally), gemcitabine (15 mg/kg body weight every 72 h intraperitoneally), and analog **84** plus gemcitabine (n = 6, per group). The tumor volume was measured every 3-days for 4-weeks by using digital calibers. Tumor volumes were determined by measuring ($1/2 \times \text{length} \times \text{width}^2$) in cubic millimeters. After the 27th day of treatment, the mice were sacrificed, and the tumor weight was determined.

4.3. Proliferation index

Vehicle and analog **84** treated subcutaneous tumor tissue were formalin-fixed, paraffin-embedded sections (5 mm) were stained with anti-Ki-67 antibody (Abcam, USA) in Tissue Science Facility, UNMC, USA. Results were expressed as percentage of Ki-67–positive cells mean ± SEM per original magnification. A total of 4 fields per tumor were examined and counted from vehicle and treated groups (n = 5). The values were subjected to unpaired Student *t*-test.

4.4. Immunohistochemistry

The paraffin-embedded vehicle and treated slides were deparaffinized with xylene, re-hydrated with series of alcohol, antigen retrieval in citrate buffer (pH = 6.0) for 10 min heating chamber and quenched with hydrogen peroxide. After blocking with a universal blocker (Thermo Fisher Scientific, USA), the slides were incubated with antibody p-IKKβ (Cell Signaling Technology, USA) overnight at 4 °C. Next day, the slides were washed and incubated with HRP conjugated secondary antibody (Dako, USA) for 1 h at room temperature. Further, the slides were washed and developed using 3,30-diaminobenzidine tetrahydrochloride (DAB, Vector Laboratories, USA) substrate. The slides were counterstained with hematoxylin, washed with water, dehydrated with alcohol series, and after xylene washes, the slides were mounted with the coverslip. Image were captured by bright field microscope (Nikon, Japan). The histological scoring was performed based on staining intensity (0, negligible; 1, low; 2, moderate; 3, high) and proportion (0%–100%). The histoscore was created by multiplying the stain proportion score (1, <5%; 2, 5%–25%; 3, 26%–50%; 4, 51%–75%; 5, >75%) with the intensity score (0–3) to obtain values between 0 and 15.

4.5. Statistical analysis

Data are presented as the average ± SEM. Live/dead cell assay was analyzed by 2-way ANOVA with Bonferroni's multiple comparisons test. Colony formation, gap closure, tumor weight, tumor volume, Ki-67 and Histoscore of p-IKKβ was analyzed by unpaired student's t-test. The p value less than 0.05 was considered statistically significant.

Declaration of competing interest

The authors declare that they have no known competing financial interests or personal relationships that could have appeared to influence the work reported in this paper.

Acknowledgement

This work was supported in part by NIH grants CA182820, CA197999, CA251151, CA208108 and CA036727. Support from the NRI-POC is also gratefully acknowledged. JIC was supported by UNMC fellowship and thank Dr. Divya Thomas for technical assistance.

Appendix A. Supplementary data

Supplementary data to this article can be found online at https://doi.org/10.1016/j.ejmech.2021.113579.

References

[1] J.A. Pereira, A.M. Pessoa, M.N. Cordeiro, R. Fernandes, C. Prudencio, J.P. Noronha, M. Vieira, Quinoxaline, its derivatives and applications: a State of the Art review, Eur. J. Med. Chem. 97 (2015) 664–672.
[2] J.W. Coe, P.R. Brooks, M.G. Vetelino, M.C. Wirtz, E.P. Arnold, J. Huang, S.B. Sands, T.I. Davis, L.A. Lebel, C.B. Fox, A. Shrikhande, J.H. Heym, E. Schaeffer, H. Rollema, Y. Lu, R.S. Mansbach, L.K. Chambers, C.C. Rovetti, D.W. Schulz, F.D. Tingley 3rd, B.T. O'Neill, Varenicline: an alpha4beta2 nicotinic receptor partial agonist for smoking cessation, J. Med. Chem. 48 (2005) 3474–3477.
[3] D. Cambridge, UK-14,304, a potent and selective alpha2-agonist for the characterisation of alpha-adrenoceptor subtypes, Eur. J. Pharmacol. 72 (1981) 413–415.
[4] M.F. Sugrue, New approaches to antiglaucoma therapy, J. Med. Chem. 40 (1997) 2793–2809.
[5] H.C. Richards, J.R. Housley, D.F. Spooner, Quinacillin: a new penicillin with unusual properties, Nature 199 (1963) 354–356.
[6] T. Pillaiyar, V. Namasivayam, M. Manickam, Macrocyclic hepatitis C virus NS3/4A protease inhibitors: an overview of medicinal chemistry, Curr. Med. Chem. 23 (2016) 3404–3447.
[7] J.A. McCauley, M.T. Rudd, Hepatitis C virus NS3/4a protease inhibitors, Curr. Opin. Pharmacol. 30 (2016) 84–92.
[8] T.P.S. Perera, E. Jovcheva, L. Mevellec, J. Vialard, D. De Lange, T. Verhulst, C. Paulussen, K. Van De Ven, P. King, E. Freyne, D.C. Rees, M. Squires, G. Saxty, M. Page, C.W. Murray, R. Gilissen, G. Ward, N.T. Thompson, D.R. Newell, N. Cheng, L. Xie, J. Yang, S.J. Platero, J.D. Karkera, C. Moy, P. Angibaud, S. Laquerre, M.V. Lorenzi, Discovery and pharmacological characterization of JNJ-42756493 (Erdafitinib), a functionally selective small-molecule FGFR family inhibitor, Mol. Canc. Therapeut. 16 (2017) 1010–1020.
[9] J.D. Karkera, G.M. Cardona, K. Bell, D. Gaffney, J.C. Portale, A. Santiago-Walker, C.H. Moy, P. King, M. Sharp, R. Bahleda, F.R. Luo, J.D. Alvarez, M.V. Lorenzi, S.J. Platero, Oncogenic characterization and pharmacologic sensitivity of activating fibroblast growth factor receptor (FGFR) genetic alterations to the selective FGFR inhibitor Erdafitinib, Mol. Canc. Therapeut. 16 (2017) 1717–1726.
[10] K.J. Addess, J. Feigon, NMR investigation of Hoogsteen base pairing in quinoxaline antibiotic–DNA complexes: comparison of 2:1 echinomycin, triostin A and [N-MeCys3,N-MeCys7] TANDEM complexes with DNA oligonucleotides, Nucleic Acids Res. 22 (1994) 5484–5491.
[11] G. Ughetto, A.H. Wang, G.J. Quigley, G.A. van der Marel, J.H. van Boom, A. Rich, A comparison of the structure of echinomycin and triostin A complexed to a DNA fragment, Nucleic Acids Res. 13 (1985) 2305–2323.
[12] T. Kaushal, G. Srivastava, A. Sharma, A. Singh Negi, An insight into medicinal chemistry of anticancer quinoxalines, Bioorg. Med. Chem. 27 (2019) 16–35.
[13] A. Simeonov, A. Yasgar, A. Jadhav, G.L. Lokesh, C. Klumpp, S. Michael, C.P. Austin, A. Natarajan, J. Inglese, Dual-fluorophore quantitative high-throughput screen for inhibitors of BRCT-phosphoprotein interaction, Anal. Biochem. 375 (2008) 60–70.
[14] G.L. Lokesh, A. Rachamallu, G.D. Kumar, A. Natarajan, High-throughput fluorescence polarization assay to identify small molecule inhibitors of BRCT domains of breast cancer gene 1, Anal. Biochem. 352 (2006) 135–141.
[15] D. Maroni, S. Rana, C. Mukhopadhyay, A. Natarajan, M. Naramura, A quinoxaline urea analog uncouples inflammatory and pro-survival functions of IKKbeta, Immunol. Lett. 168 (2015) 319–324.
[16] P. Radhakrishnan, V.C. Bryant, E.C. Blowers, R.N. Rajule, N. Gautam, M.M. Anwar, A.M. Mohr, P.M. Grandgenett, S.K. Bunt, J.L. Arnst, S.M. Lele, Y. Alnouti, M.A. Hollingsworth, A. Natarajan, Targeting the NF-kappaB and mTOR pathways with a quinoxaline urea analog that inhibits IKKbeta for pancreas cancer therapy, Clin. Canc. Res. 19 (2013) 2025–2035.
[17] N. Gautam, S.P. Bathena, Q. Chen, A. Natarajan, Y. Alnouti, Pharmacokinetics, protein binding and metabolism of a quinoxaline urea analog as an NF-kappaB inhibitor in mice and rats by LC-MS/MS, Biomed. Chromatogr. 27 (2013) 900–909.
[18] N.K. Chaturvedi, R.N. Rajule, A. Shukla, P. Radhakrishnan, G.L. Todd, A. Natarajan, J.M. Vose, S.S. Joshi, Novel treatment for mantle cell lymphoma including therapy-resistant tumor by NF-kappaB and mTOR dual-targeting approach, Mol. Canc. Therapeut. 12 (2013) 2006–2017.
[19] R. Rajule, V.C. Bryant, H. Lopez, X. Luo, A. Natarajan, Perturbing pro-survival proteins using quinoxaline derivatives: a structure-activity relationship study, Bioorg. Med. Chem. 20 (2012) 2227–2234.
[20] Q. Chen, V.C. Bryant, H. Lopez, D.L. Kelly, X. Luo, A. Natarajan, 2,3-Substituted quinoxalin-6-amine analogs as antiproliferatives: a structure-activity relationship study, Bioorg. Med. Chem. Lett 21 (2011) 1929–1932.
[21] J.V. Napoleon, S. Singh, S. Rana, M. Bendjennat, V. Kumar, S. Kizhake, N.Y. Palermo, M.M. Ouellette, T. Huxford, A. Natarajan, Small molecule binding to inhibitor of nuclear factor kappa-B kinase subunit beta in an ATP non-competitive manner, Chem. Commun. 57 (2021) 4678–4681.
[22] F. Liu, Y. Xia, A.S. Parker, I.M. Verma, IKK biology, Immunol. Rev. 246 (2012) 239–253.
[23] J.A. DiDonato, F. Mercurio, M. Karin, NF-kappaB and the link between inflammation and cancer, Immunol. Rev. 246 (2012) 379–400.
[24] A. Israel, The IKK complex, a central regulator of NF-kappaB activation, Cold Spring Harb Perspect Biol 2 (2010) a000158.
[25] D.F. Lee, H.P. Kuo, C.T. Chen, J.M. Hsu, C.K. Chou, Y. Wei, H.L. Sun, L.Y. Li, B. Ping, W.C. Huang, X. He, J.Y. Hung, C.C. Lai, Q. Ding, J.L. Su, J.Y. Yang, A.A. Sahin, G.N. Hortobagyi, F.J. Tsai, C.H. Tsai, M.C. Hung, IKK beta suppression of TSC1 links inflammation and tumor angiogenesis via the mTOR pathway, Cell 130 (2007) 440–455.
[26] E. Maniati, M. Bossard, N. Cook, J.B. Candido, N. Emami-Shahri, S.A. Nedospasov, F.R. Balkwill, D.A. Tuveson, T. Hagemann, Crosstalk between the canonical NF-kappaB and Notch signaling pathways inhibits Ppargamma expression and promotes pancreatic cancer progression in mice, J. Clin. Invest. 121 (2011) 4685–4699.
[27] J. Ling, Y. Kang, R. Zhao, Q. Xia, D.F. Lee, Z. Chang, J. Li, B. Peng, J.B. Fleming, H. Wang, J. Liu, I.R. Lemischka, M.C. Hung, P.J. Chiao, KrasG12D-induced IKK2/beta/NF-kappaB activation by IL-1alpha and p62 feedforward loops is required for development of pancreatic ductal adenocarcinoma, Canc. Cell 21 (2012) 105–120.
[28] Y. Xia, N. Yeddula, M. Leblanc, E. Ke, Y. Zhang, E. Oldfield, R.J. Shaw, I.M. Verma, Reduced cell proliferation by IKK2 depletion in a mouse lung-cancer model, Nat. Cell Biol. 14 (2012) 257–265.
[29] K. Vlantis, A. Wullaert, Y. Sasaki, M. Schmidt-Supprian, K. Rajewsky, T. Roskams, M. Pasparakis, Constitutive IKK2 activation in intestinal epithelial cells induces intestinal tumors in mice, J. Clin. Invest. 121 (2011) 2781–2793.
[30] H. Shaked, L.J. Hofseth, A. Chumanevich, A.A. Chumanevich, J. Wang, Y. Wang, K. Taniguchi, M. Guma, S. Shenouda, H. Clevers, C.C. Harris, M. Karin, Chronic epithelial NF-kappaB activation accelerates APC loss and intestinal tumor initiation through iNOS up-regulation, Proc. Natl. Acad. Sci. U. S. A. 109 (2012) 14007–14012.
[31] M. Naramura, A. Natarajan, Mouse pancreatic tumor model independent of tumor suppressor gene inactivation, Pancreas 47 (2018) e27–e29.
[32] H. Suzuki, T. Chiba, M. Kobayashi, M. Takeuchi, T. Suzuki, A. Ichiyama, T. Ikenoue, M. Omata, K. Furuichi, K. Tanaka, IkappaBalpha ubiquitination is catalyzed by an SCF-like complex containing Skp1, cullin-1, and two F-box/WD40-repeat proteins, betaTrCP1 and betaTrCP2, Biochem. Biophys. Res. Commun. 256 (1999) 127–132.
[33] M. Kroll, F. Margottin, A. Kohl, P. Renard, H. Durand, J.P. Concordet, F. Bachelerie, F. Arenzana-Seisdedos, R. Benarous, Inducible degradation of IkappaBalpha by the proteasome requires interaction with the F-box protein h-betaTrCP, J. Biol. Chem. 274 (1999) 7941–7945.
[34] B. Tian, D.E. Nowak, M. Jamaluddin, S. Wang, A.R. Brasier, Identification of direct genomic targets downstream of the nuclear factor-kappaB transcription factor mediating tumor necrosis factor signaling, J. Biol. Chem. 280 (2005) 17435–17448.
[35] B. Tian, D.E. Nowak, A.R. Brasier, A TNF-induced gene expression program under oscillatory NF-kappaB control, BMC Genom. 6 (2005) 137.
[36] T.D. Gilmore, M. Herscovitch, Inhibitors of NF-kappaB signaling: 785 and counting, Oncogene 25 (2006) 6887–6899.
[37] M.L. de Castro Barbosa, R.A. da Conceicao, A.G.M. Fraga, B.D. Camarinha, G.C. de Carvalho Silva, A.G.F. Lima, E.A. Cardoso, V. de Oliveira Freitas Lione, NF-kappaB signaling pathway inhibitors as anticancer drug candidates, Anticancer Agents Med Chem 17 (2017) 483–490.
[38] V. Ramadass, T. Vaiyapuri, V. Tergaonkar, Small molecule NF-kappaB pathway inhibitors in clinic, Int. J. Mol. Sci. 21 (2020).
[39] B. Gatto, Biologics targeted at TNF: design, production and challenges, Reumatismo 58 (2006) 94–103.
[40] S. Rana, E.C. Blowers, C. Tebbe, J.I. Contreras, P. Radhakrishnan, S. Kizhake, T. Zhou, R.N. Rajule, J.L. Arnst, A.R. Munkarah, R. Rattan, A. Natarajan, Isatin derived spirocyclic analogues with alpha-Methylene-gamma-butyrolactone as anticancer agents: a structure-activity relationship study, J. Med. Chem. 59 (2016) 5121–5127.
[41] V.C. Bryant, G.D. Kishore Kumar, A.M. Nyong, A. Natarajan, Synthesis and evaluation of macrocyclic diarylether heptanoid natural products and their analogs, Bioorg. Med. Chem. Lett 22 (2012) 245–248.

[42] D. Wen, Y. Nong, J.G. Morgan, P. Gangurde, A. Bielecki, J. Dasilva, M. Keaveney, H. Cheng, C. Fraser, L. Schopf, M. Hepperle, G. Harriman, B.D. Jaffee, T.D. Ocain, Y. Xu, A selective small molecule IkappaB Kinase beta inhibitor blocks nuclear factor kappaB-mediated inflammatory responses in human fibroblast-like synoviocytes, chondrocytes, and mast cells, J. Pharmacol. Exp. Therapeut. 317 (2006) 989–1001.
[43] P.L. Podolin, J.F. Callahan, B.J. Bolognese, Y.H. Li, K. Carlson, T.G. Davis, G.W. Mellor, C. Evans, A.K. Roshak, Attenuation of murine collagen-induced arthritis by a novel, potent, selective small molecule inhibitor of IkappaB Kinase 2, TPCA-1 (2-[(aminocarbonyl)amino]-5-(4-fluorophenyl)-3-thiophenecarboxamide), occurs via reduction of proinflammatory cytokines and antigen-induced T cell Proliferation, J. Pharmacol. Exp. Therapeut. 312 (2005) 373–381.
[44] J.R. Burke, M.A. Pattoli, K.R. Gregor, P.J. Brassil, J.F. MacMaster, K.W. McIntyre, X. Yang, V.S. Iotzova, W. Clarke, J. Strnad, Y. Qiu, F.C. Zusi, BMS-345541 is a highly selective inhibitor of I kappa B kinase that binds at an allosteric site of the enzyme and blocks NF-kappa B-dependent transcription in mice, J. Biol. Chem. 278 (2003) 1450–1456.
[45] K. Nagashima, V.G. Sasseville, D. Wen, A. Bielecki, H. Yang, C. Simpson, E. Grant, M. Hepperle, G. Harriman, B. Jaffee, T. Ocain, Y. Xu, C.C. Fraser, Rapid TNFR1-dependent lymphocyte depletion in vivo with a selective chemical inhibitor of IKKbeta, Blood 107 (2006) 4266–4273.
[46] F.R. Greten, M.C. Arkan, J. Bollrath, L.C. Hsu, J. Goode, C. Miething, S.I. Goktuna, M. Neuenhahn, J. Fierer, S. Paxian, N. Van Rooijen, Y. Xu, T. O'Cain, B.B. Jaffee, D.H. Busch, J. Duyster, R.M. Schmid, L. Eckmann, M. Karin, NF-kappaB is a negative regulator of IL-1beta secretion as revealed by genetic and pharmacological inhibition of IKKbeta, Cell 130 (2007) 918–931.
[47] S. Rana, A. Natarajan, Face selective reduction of the exocyclic double bond in isatin derived spirocyclic lactones, Org. Biomol. Chem. 11 (2013) 244–247.
[48] E.A. Kumar, Q. Chen, S. Kizhake, C. Kolar, M. Kang, C.E. Chang, G.E. Borgstahl, A. Natarajan, The paradox of conformational constraint in the design of Cbl(TKB)-binding peptides, Sci. Rep. 3 (2013) 1639.
[49] A. Natarajan, Y. Guo, H. Arthanari, G. Wagner, J.A. Halperin, M. Chorev, Synthetic studies toward aryl-(4-aryl-4H-[1,2,4]triazole-3-yl)-amine from 1,3-diarylthiourea as urea mimetics, J. Org. Chem. 70 (2005) 6362–6368.
[50] J. Deng, E. Feng, S. Ma, Y. Zhang, X. Liu, H. Li, H. Huang, J. Zhu, W. Zhu, X. Shen, L. Miao, H. Liu, H. Jiang, J. Li, Design and synthesis of small molecule RhoA inhibitors: a new promising therapy for cardiovascular diseases? J. Med. Chem. 54 (2011) 4508–4522.
[51] D. Ray, A.M. Nyong, A. Natarajan, Synthesis of unnatural amino acid derivatives via palladium catalyzed 1,4 addition of boronic acids, Tetrahedron Lett. 51 (2010) 2655–2656.
[52] C.M. Robb, S. Kour, J.I. Contreras, E. Agarwal, C.J. Barger, S. Rana, Y. Sonawane, B.K. Neilsen, M. Taylor, S. Kizhake, R.N. Thakare, S. Chowdhury, J. Wang, J.D. Black, M.A. Hollingsworth, M.G. Brattain, A. Natarajan, Characterization of CDK(5) inhibitor, 20-223 (aka CP668863) for colorectal cancer therapy, Oncotarget 9 (2018) 5216–5232.
[53] J.I. Contreras, C.M. Robb, H.M. King, J. Baxter, A.J. Crawford, S. Kour, S. Kizhake, Y.A. Sonawane, S. Rana, M.A. Hollingsworth, X. Luo, A. Natarajan, Chemical genetic screens identify kinase inhibitor combinations that target anti-apoptotic proteins for cancer therapy, ACS Chem. Biol. 13 (2018) 1148–1152.
[54] S. Kour, S. Rana, J.I. Contreras, H.M. King, C.M. Robb, Y.A. Sonawane, M. Bendjennat, A.J. Crawford, C.J. Barger, S. Kizhake, X. Luo, M.A. Hollingsworth, A. Natarajan, CDK5 inhibitor downregulates mcl-1 and sensitizes pancreatic cancer cell lines to navitoclax, Mol. Pharmacol. 96 (2019) 419–429.
[55] P. Smolewski, J. Grabarek, H.D. Halicka, Z. Darzynkiewicz, Assay of caspase activation in situ combined with probing plasma membrane integrity to detect three distinct stages of apoptosis, J. Immunol. Methods 265 (2002) 111–121.
[56] N.A. Franken, H.M. Rodermond, J. Stap, J. Haveman, C. van Bree, Clonogenic assay of cells in vitro, Nat. Protoc. 1 (2006) 2315–2319.
[57] D. Thomas, P. Radhakrishnan, Tumor-stromal crosstalk in pancreatic cancer and tissue fibrosis, Mol. Canc. 18 (2019) 14.
[58] L.A. Peterson, Reactive metabolites in the biotransformation of molecules containing a furan ring, Chem. Res. Toxicol. 26 (2013) 6–25.
[59] C.A. Lipinski, F. Lombardo, B.W. Dominy, P.J. Feeney, Experimental and computational approaches to estimate solubility and permeability in drug discovery and development settings, Adv. Drug Deliv. Rev. 46 (2001) 3–26.
[60] S. Rana, Y.A. Sonawane, M.A. Taylor, S. Kizhake, M. Zahid, A. Natarajan, Synthesis of aminopyrazole analogs and their evaluation as CDK inhibitors for cancer therapy, Bioorg. Med. Chem. Lett 28 (2018) 3736–3740.
[61] S. Rana, S. Kour, Y.A. Sonawane, C.M. Robb, J.I. Contreras, S. Kizhake, M. Zahid, A.R. Karpf, A. Natarajan, Symbiotic prodrugs (SymProDs) dual targeting of NFkappaB and CDK, Chem. Biol. Drug Des. 96 (2020) 773–784.